

Transport, non-locality, & Large Scale Dynamamos: Challenges for For Next Generation Accretion Theory

Eric Blackman (U. Rochester)

Prologue:

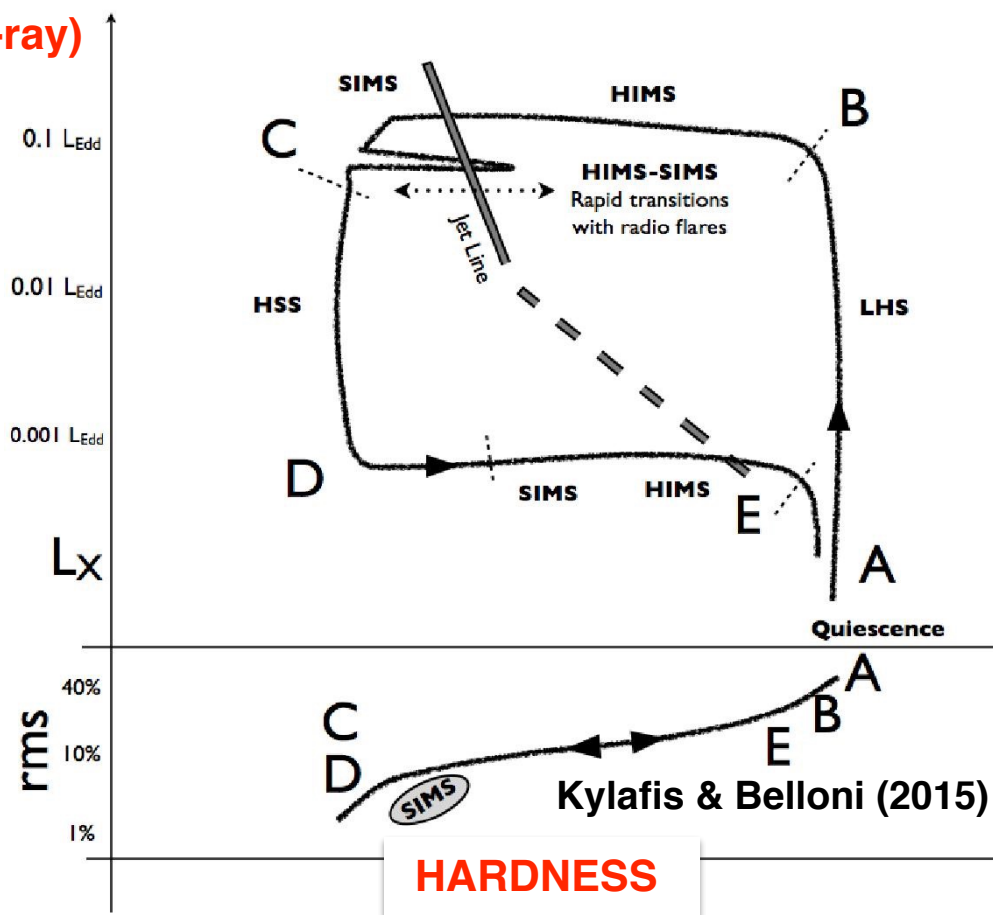
- Magnetic fields are likely key agents of transport in accreting systems and mediators of associated particle acceleration
- That magnetic fields are mainstays throughout astrophysics traces back to early radio astronomy (Jansky 1932, and into 1940s) and puzzles it posed.
- In laboratory context: synchrotron radiation was measured in lab 1947 (General Electric electron accelerator) and Ginzburg (1947) proposed the “undulator”, now a mainstay of synchrotron lab sources
- Ginzburg was central to bridging the gap between synchrotron theory (e.g. Schott 1912; Pomeranchuk 1938...) and astrophysical contexts
- Tracing the history, Ginzburg (1965, 1985) cites early key papers Alfvén & Herlofson 1950 (stars) and Kippenheuer 1950, Ginzburg 1951 (galactic ISM synchrotron)
- Ginzburg & Syrovatskii (1965, ARAA):

At any rate, at the Paris symposium on radio astronomy in 1958 (cf. 48), in contrast to the Manchester symposium in 1955 (cf. 40), the magnetobremstrahlung theory of nonthermal cosmic radio emission was already generally accepted.

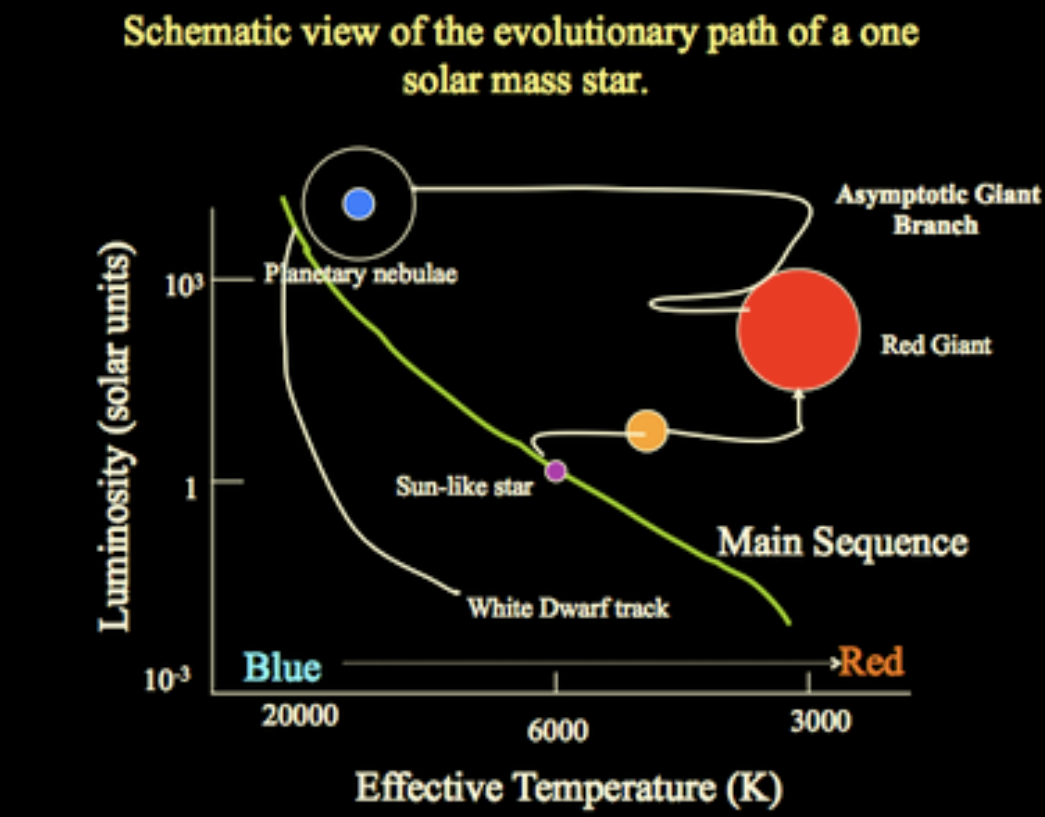
A Grand Challenge For Accretion Theory: *Explain luminosity, spectra, disk morphology, and time evolution of engines surrounding stellar and compact objects to a level comparable to that of stellar evolution theory.*

LUMINOSITY (x-ray)

Microquasar Accretion Evolution

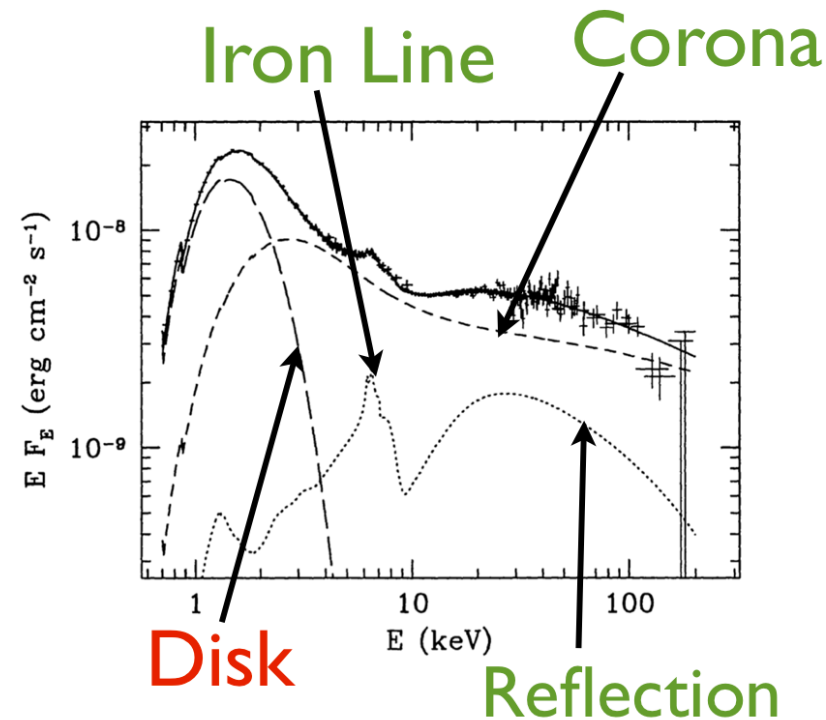


Stellar Evolution (H-R Diagram)



What's Missing from Present Disk Modeling

- Disk spectra are ubiquitously modeled with standard (incredibly practical) Shakura-Sunyaev (1973)-type disk “glued” to other components
- “Practical” models use “viscous” transport prescription with constant “alpha”; $\nu = \alpha_{ss} c_s H$
- Simulations until recently, have largely focused on local transport (that is changing) and local simulations can't capture non-local transport (note Lynden-Bell '69).
- Little feedback between decades of simulations and improving theory



Cyg X-1 (X-ray binary, [Gierlinski & Zdziarski 99](#))

- How much transport is local vs. non-local ?
- How do the magnetic fields, which influence transport, emerge self-consistently?
- **Next-generation theory should:** (i) explain how disk, coroneae, and jet contributions arise in their respective proportions (ii) capture the physics of transport beyond viscous assumption (iii) explain origin of field

Standard “Viscous” Approximation Highlights Opportunity

- Axisymmetry is incompatible with ‘turbulence’ unless a property of averaged equations; standard disk theory is thus necessarily a **mean field theory**
- Assumption of “viscous” transport and computational limitations has led to use of local “shearing box” models to study the role of magnetic fields particularly the magneto-rotational instability (MRI) (Velikhov 1959) as applied to accretion disks (Balbus & Hawley 1991 + etc.....)
- Even if MRI were dominant, this does not imply that transport is local: How MRI stress saturates and on what scales is important to address: MRI can, and does generate large scale fields
- The multiple components of the mean stresses not

$$\nabla \cdot \left[r \rho v_\phi \mathbf{v} - r B_\phi \mathbf{B}_p + r \left(P + \frac{B_p^2}{8\pi} \right) \mathbf{e}_\phi \right] = \nabla \cdot \mathbf{F} \quad \leftarrow \text{macrophysical contribution to flux divergence in steady-state angular momentum density evolution equation}$$

$$F_{r\phi} = \left[r \rho v_\phi v_r - r \frac{B_\phi}{4\pi} B_r \right]$$

$$\bar{F}_{r\phi,\pm} = \frac{\Sigma r}{2H} \left[\bar{V}_\phi \bar{V}_r - \bar{V}_{A\phi} \bar{V}_{Ar} + \langle v_r v_\phi \rangle - \langle v_{Ar} v_{A\phi} \rangle \right]_{\pm}$$

$$\bar{F}_{\phi z,\pm} = \frac{\Sigma r}{2H} \left[\bar{V}_\phi \bar{V}_z - \bar{V}_{A\phi} \bar{V}_{Az} + \langle v_\phi v_z \rangle - \langle v_{A\phi} v_{Az} \rangle \right]_{\pm}$$

Local Cartesian approx:

$$\begin{aligned} \bar{W}_{xy} &\equiv \langle v_x v_y \rangle - \langle v_{Ax} v_{Ay} \rangle = -v_{\text{eff}} (r \partial_r \Omega)_{r=r_0} = v_{\text{eff}} q \Omega \\ &= (\alpha_{ss} c_s H) q \Omega ; \quad q \equiv d \ln \Omega / d \ln r \\ &= \alpha_{ss} q c_s^2 \end{aligned}$$

Mass
Accretion

Coronal
Stress

Disk turbulence;
radial, azimuthal

Outflow
Stress

Disk turbulence;
vertical, azimuthal

Note also linear dependence on q

Indications of non-local transport

- jets, outflows, and coronae are ubiquitous
- Seyfert AGN: ~30% of bolometric emission from X-rays Mushotzky et al. 93, likely low plasma β coronae: Perhaps only field structures with large enough scale for turbulent shredding time to exceed buoyancy time contribute (Blackman & Pessah 09)
- coupling between disk, star, stellar magnetosphere (e.g. Matt & Pudritz 2005; Li et al. 2012 Romanova et al. 2012; Romanova et al. 2011,2012,2013,2017)
- non-radiation pressure dominated simulations saturate with $\alpha * \beta = \text{constant}$ (e.g. Blackman et al. 2006); Some observations of DN, and AGN require $\alpha=0.1$ (King et al. 2007) and such large α can arise in simulations with strong initial large scale fields in local sims (Bai & Stone 2013) or global simulations dominated by large scale transport (Zhu & Stone 2017);
- Ghisellini et al. 2014: Blazars have more power in outflows than disk allows, suggesting that accretion must supply a large scale field to hole for jet extraction (via Blandford-Znajek) Note also Star-Disk Collision driven AGN dynamos (Pariev et al. 2007)
- [Note: In YSOs, large scale disk structures now observed with ALMA Cassius et al (13); van der Marel et al. (2013..+); vortices, self-gravity, and planets, spiral waves, dead zone and winds make YSO complicated, and NL transport is already conspicuous in fully ionized systems]

Even “local” simulations hint toward not purely viscous, non-local transport; global simulations agree

- Shearing box (with all its maladies) is best regarded as a controlled physics experiment not a representation of astrophysical system but even they show importance of non-local, non-viscous transport (e.g. Blackman & Nauman 2015 rev,)
- **“Large/System” scales dominate the stresses** in both shearing boxes and global simulations (e.g. Beckwith et al. 11, Zhu & Stone 17) where large scale coronal torques dominate overall accretion
- stress not linearly proportional to shear (Abramowicz et al. 1996; Pessah et al. 2006; Penna et al. 2013; Nauman Blackman 2015;; Zhu & Stone 2017) and varies with radius
- **Large/System scale dynamo cycle periods correlate with stress** (LSDs): prevalent in local MRI simulations:
 - *Unstratified* tall (Lesur & Ogilvie 2008; Shi et al. 2016.)
 - Stratified (Brandenburg 1996; Davis et al 2010; Bai & Stone 2013; Nauman & B. 2014; Ebrahimi & Blackman 2016; Bhat et al. 2016..)
- **Saturation of MRI correlates with large scale dynamo saturation** (Ebrahimi 2009; Guan & Gammie 2011; Ebrahimi & Bhattacharjee 2014; Ebrahimi & Blackman 2016; Shi et al 2016)
- **Coronal fields radially correlated over large scales** $>10H$ (Guan & Gammie 2011, Zhu & Stone 2017)

Example of MRI stress dominated by system scales in shearing box

(Nauman & Blackman, 2014, BN 2015)

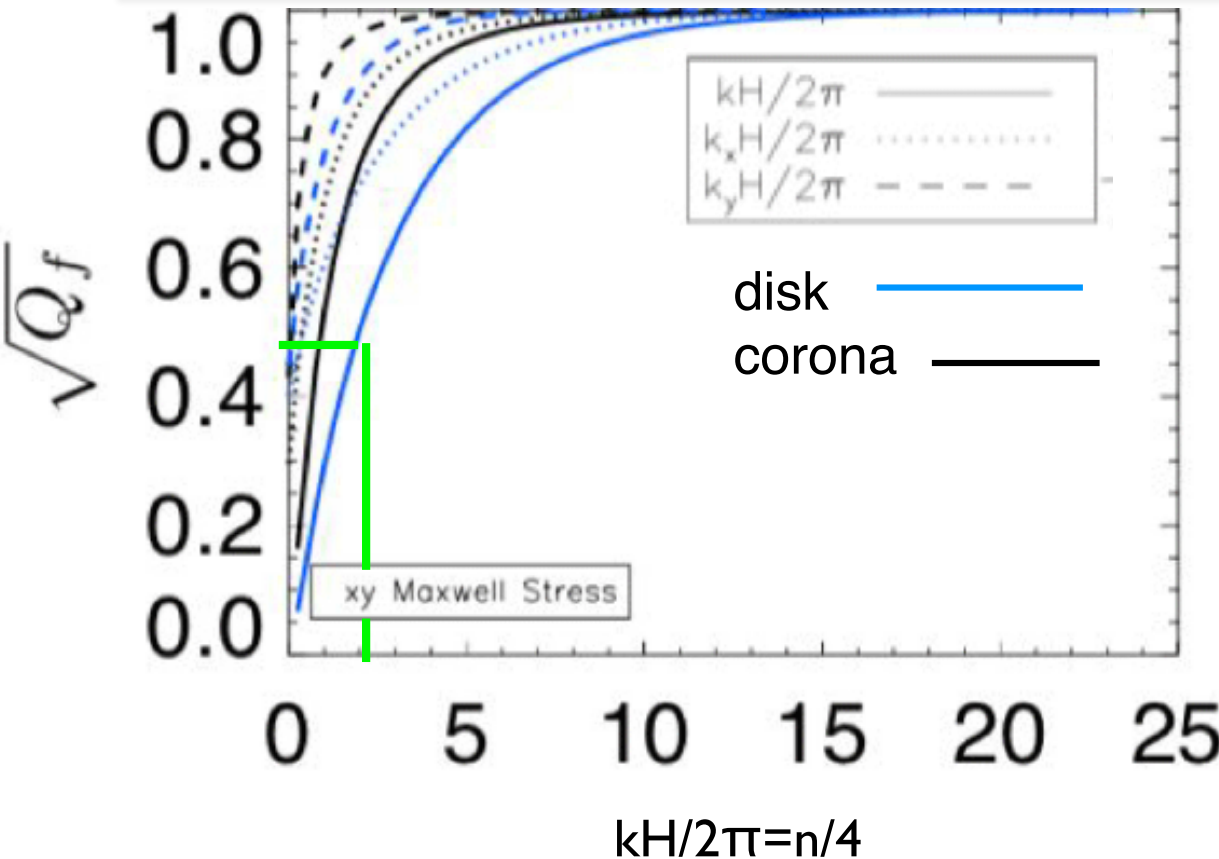
Cumulative Maxwell stress dominated by lowest modes (2-D (x,y) Fourier Trans. averaged in z)

$$Q_f(k) = \frac{\int_{k_{min}}^k |f(k')|^2 2\pi k' dk'}{\int_{k_{min}}^{k_{max}} |f(k')|^2 2\pi k' dk'}$$

$$Q_f(k_x) = \frac{\int_{k_{y,min}}^{k_y} |f(\mathbf{k})|^2 dk_y / \int dk_y}{\int_{k_{y,min}}^{k_{y,max}} |f(\mathbf{k})|^2 dk_y / \int dk_y}$$

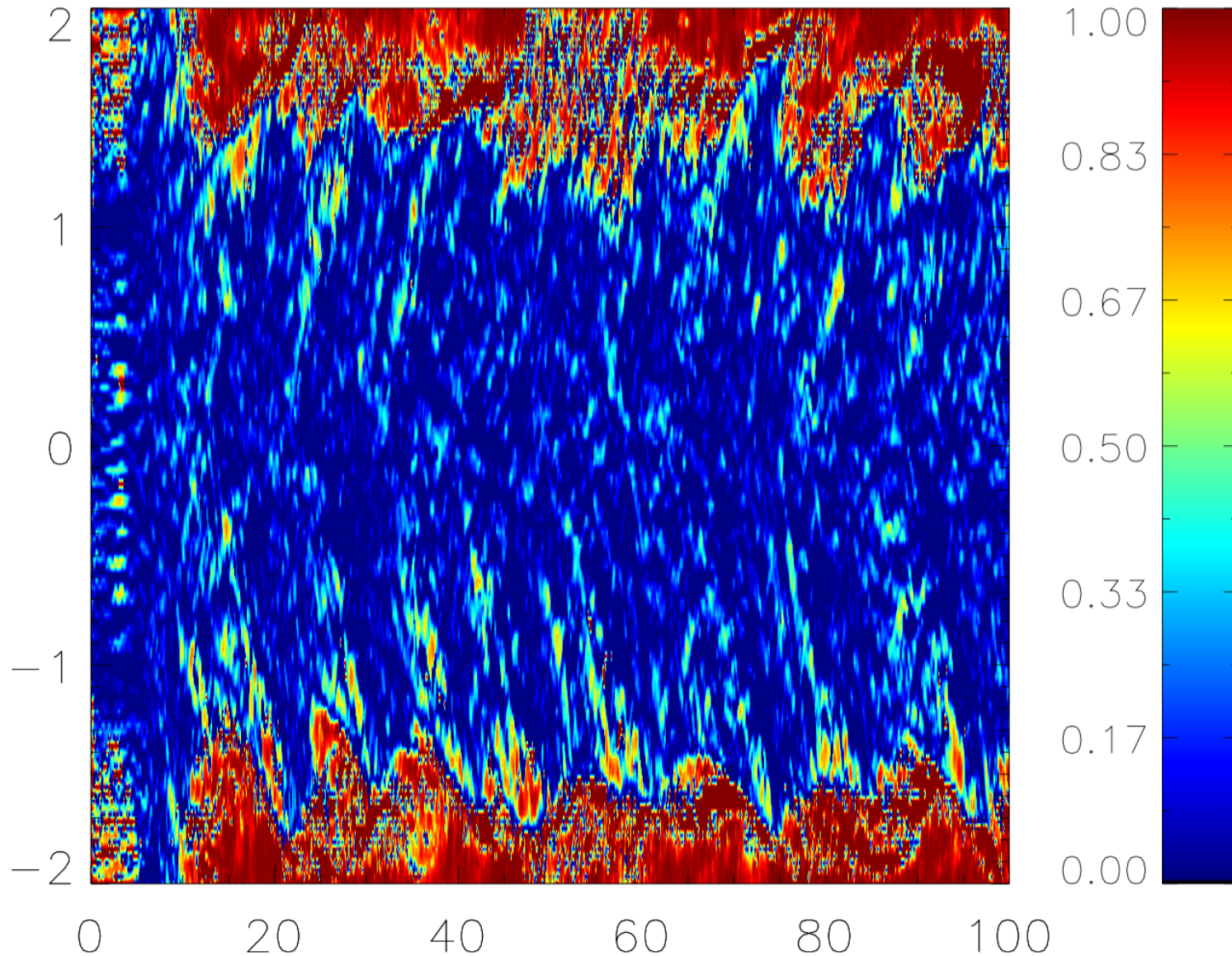
$$Q_f(k_y) = \frac{\int_{k_{x,min}}^{k_x} |f(\mathbf{k})|^2 dk_x / \int dk_x}{\int_{k_{x,min}}^{k_{x,max}} |f(\mathbf{k})|^2 dk_x / \int dk_x}$$

Isothermal, stratified, y,z-periodic; x-shear periodic; 4H x 4H x 8H; 48 zones per H; (Athena); k=2πn/L, L=4H



- consistent with emerging messages from global simulations (Beckwith et al. 2011; Sorathia et al. 2012; Parkin & Bicknell 2013..Zhu & Stone 2017)

MRI Stress Dominated by Mean Fields In corona



$$\frac{\langle B_x \rangle(z) \langle B_y \rangle(z)}{\langle B_x B_y \rangle(z)}$$

Nauman and Blackman
(2015); B2015

System/Large Scale Dynamos PRECEDE MRI turbulence in MRI unstable systems

- Planar averaged mean fields (either vertically or horizontally averaged) grow before mode-mode coupling ensues: i.e. **MRI drives large scale dynamo that PRECEDES turbulence** (Ebrahimi & Blackman 2016 (analytic, for cylinder, and local cartesian); Bhat et al. 2016 (DNS, shearing box))
- Planar averaged are sustained in the non-linear state
- Mean fields can be modeled by theory with electromotive force: fluctuations grow by MRI, and supply $\langle \mathbf{v} \times \mathbf{b} \rangle$ whose curl grows the (planar averaged) mean fields
- Non-axisymmetric perturbations are required & likely coming from a local current helicity (not kinetic helicity)

Growing large scale fields before saturation of MRI

Bhat et al. 2016

Isothermal, unstratified,
y,z-periodic; x-shear
periodic; $H \times 4H \times H$;
256 \times 1024 \times 256;
Pencil code; $\text{Pr}_M=4$
 $\text{Rm}=1250$;
 $k_x=2\pi/H$
 $k_{\text{max}}/k_l=5$

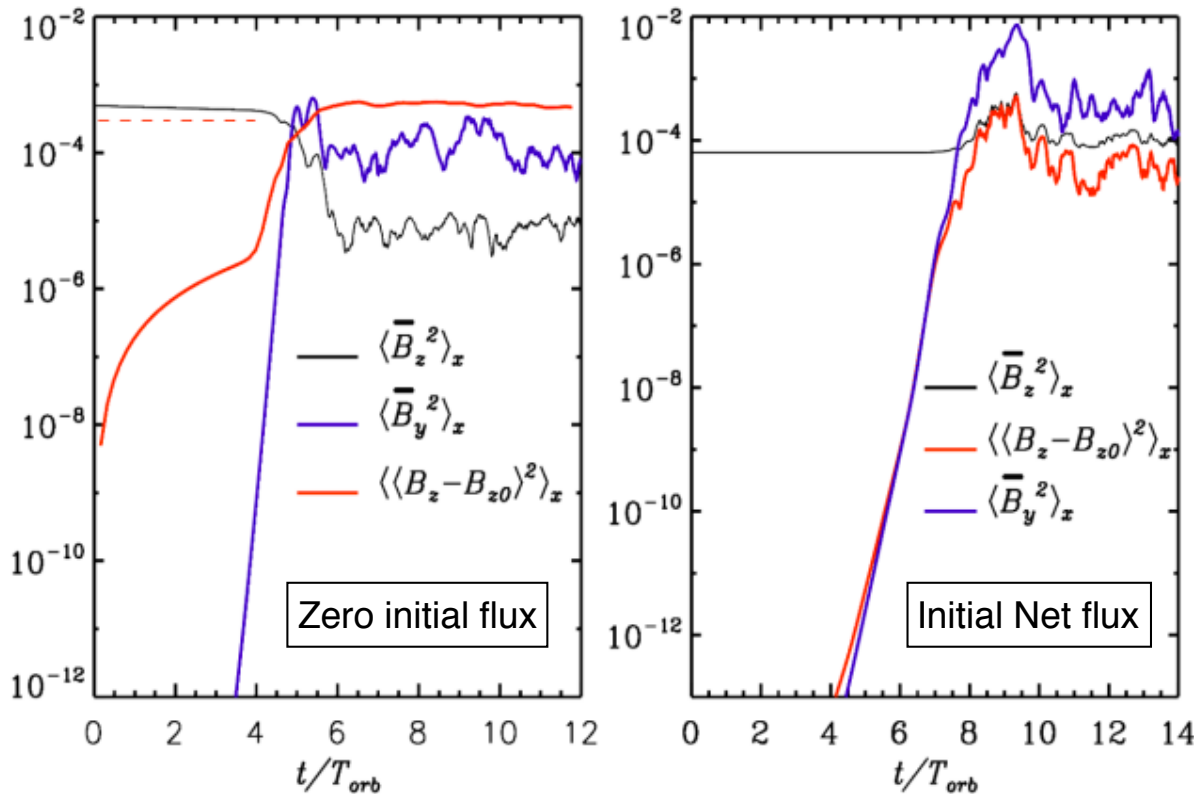
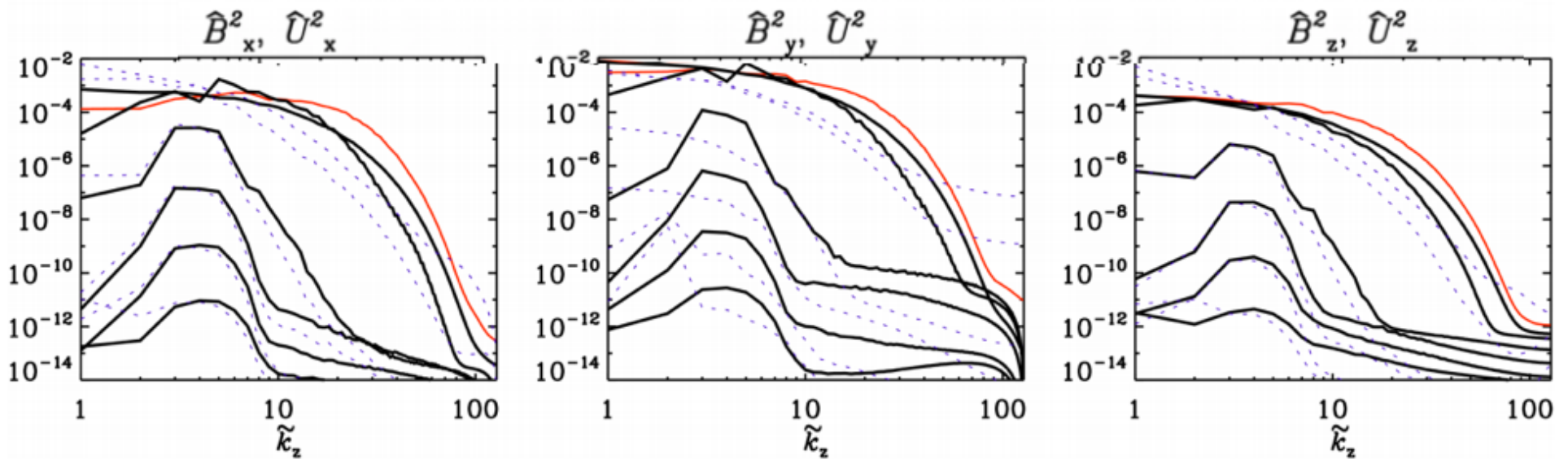


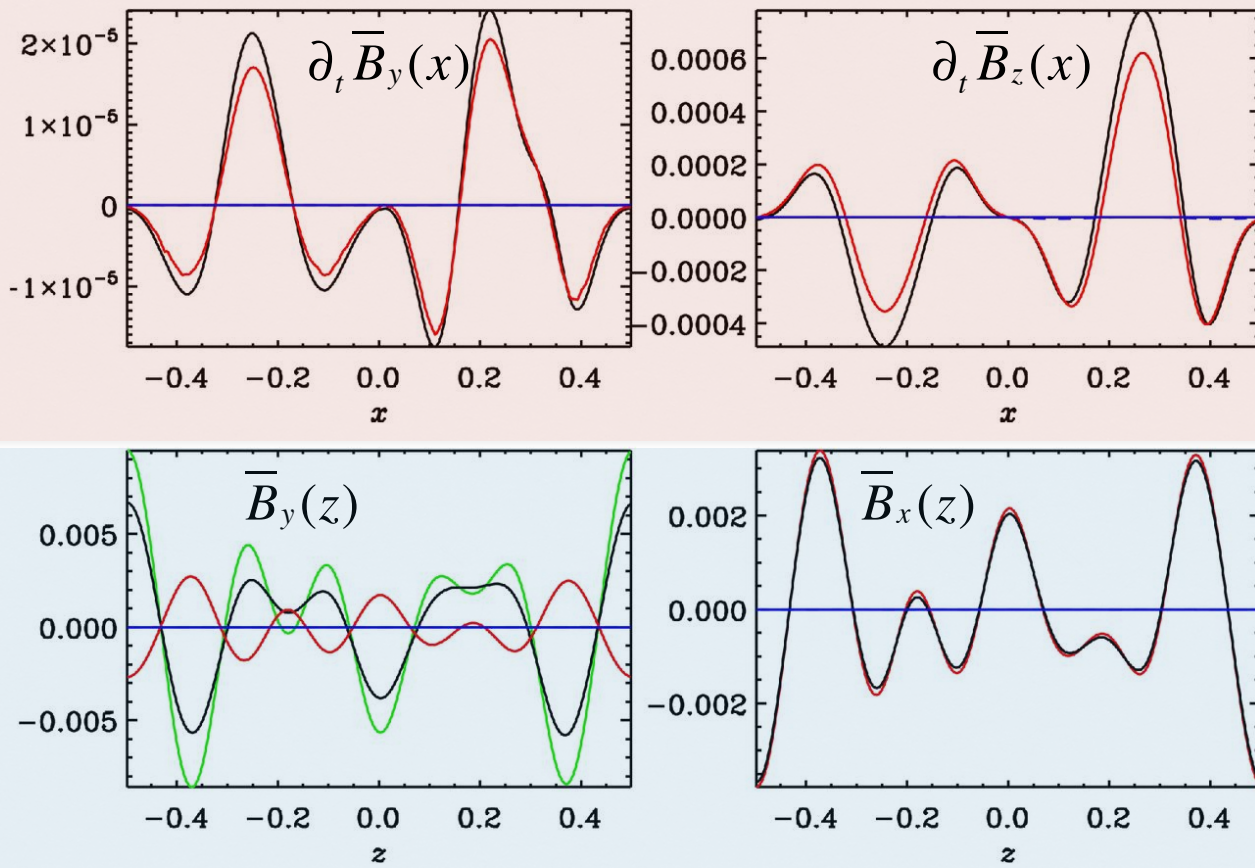
Figure 6. We show here the evolution of the mean square of y-z averaged mean fields. In the left-hand panel, the solid black line shows the total \bar{B}_z^2 and blue line shows \bar{B}_y^2 for Run A. The red dashed line indicates the slope expected for resistive decay of the field at $\tilde{k}_x = 1$ (also the initial field). The solid red line is for the quantity $\langle (\bar{B}_z - \bar{B}_{z0})^2 \rangle_x$. In the right-hand panel, \bar{B}_z^2 and \bar{B}_y^2 are shown in red and blue lines for a run where the initial field is an imposed constant and uniform mean field $B_0 = 0.008$. Additionally, we show the curve for $\langle \bar{B}_z - B_0 \rangle_x^2$, indicating growth of mean field independent

Vertically averaged mean field $\langle \bar{B}_y^2 \rangle_x$ grows at rate 2x that of the maximum growing MRI mode: Consistent with analytic quasi-linear theory (Ebrahimi & Blackman 16)

- 1-D Power spectra show that large scale fields lead growth of power on small scales before saturation



The spectra in each panel are shown in equidistant time intervals, $t/T_{\text{orb}}=1.58, 2.38, 3.18, 3.98, 4.78, 5.58$. The field saturates by $t/T_{\text{orb}} \sim 5$. And the final curve in saturated regime for \hat{B} is shown in red. Particularly in the last row, note that the spectra are initially peaked at $3 \leq \tilde{k}_z \leq 4$, which is nearly $u_{A,0}/\Omega_0$, in the MRI growth phase.



Pre-Saturation
 $t/T_{\text{orb}}=4$

Comparing Growth vs. Mean Field Equations

Time derivative of Mean Magnetic Field

Corresponding EMF terms

Linear Shear Term

Figure 7. The top two panels show the terms from y - z averaged mean field equation for $\overline{B}_y(x)$ and $\overline{B}_z(x)$ on left and right, respectively. The bottom two panels show the terms from x - y averaged mean field equation for $\overline{B}_y(z)$ and $\overline{B}_x(z)$ on left and right, respectively. These are plotted at $t/T_{\text{orb}} \sim 4$, in the MRI growth phase. The solid black curve is for the time derivative of the mean field, the red curve is for the corresponding EMF term, the green curve is for the term $S\overline{B}_x$ and the blue solid and dashed lines are, respectively, for the advection and stretching terms involving mean fields.

Vertically Averaged

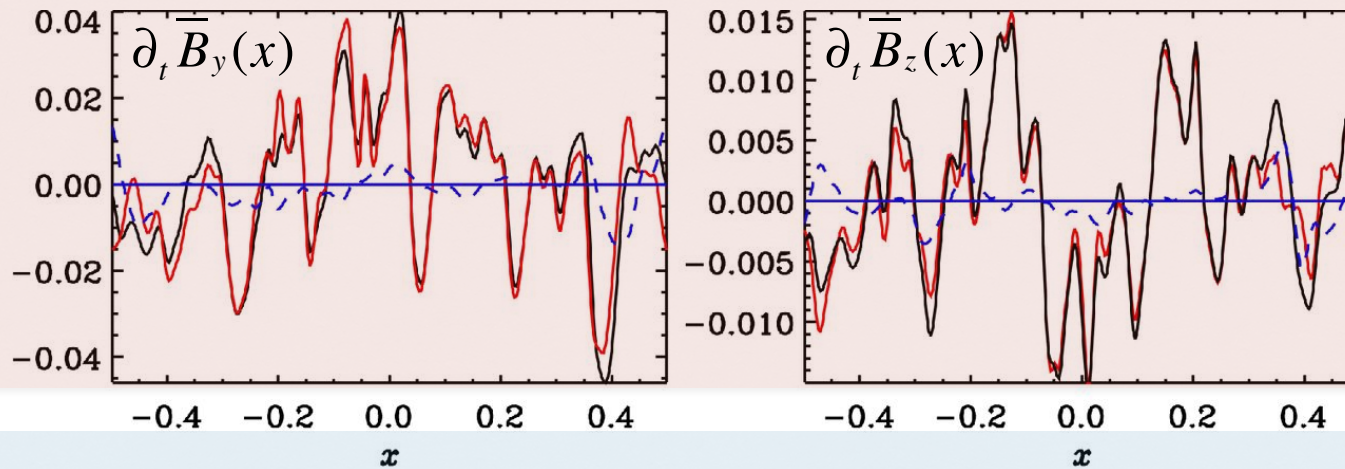
$$\frac{\partial \overline{B}_x}{\partial t} = -\partial_z \mathcal{E}_y + \overline{B}_z \partial_z \overline{U}_x - \overline{U}_z \partial_z \overline{B}_x,$$

$$\frac{\partial \overline{B}_y}{\partial t} = S\overline{B}_x + \partial_z \mathcal{E}_x + \overline{B}_z \partial_z \overline{U}_y - \overline{U}_z \partial_z \overline{B}_y,$$

Horizontally Averaged

$$\frac{\partial \overline{B}_y}{\partial t} = -\partial_x \mathcal{E}_z + \overline{B}_x \partial_x \overline{U}_y - \overline{U}_x \partial_x \overline{B}_y,$$

$$\frac{\partial \overline{B}_z}{\partial t} = \partial_x \mathcal{E}_y + \overline{B}_x \partial_x \overline{U}_z - \overline{U}_x \partial_x \overline{B}_z. \quad (17)$$



Post-Saturation
 $t/T_{\text{orb}}=19$

Comparing Growth vs. Mean Field Equations

Time evolution of Mean Magnetic Field

Corresponding EMF terms

Linear Shear Term

Figure 8. The top two panels show the terms from y - z averaged mean field equation for $\bar{B}_y(x)$ and $\bar{B}_z(x)$ on left and right, respectively. The bottom two panels show the terms from x - y averaged mean field equation for $\bar{B}_y(z)$ and $\bar{B}_x(z)$ on left and right, respectively. These are plotted at $t/T_{\text{orb}} \sim 19$, in the MRI saturation phase. The solid black curve is for the time derivative of the mean field, the red curve is for the corresponding EMF term, the green curve is for the term $S\bar{B}_x$ and the blue solid and dashed lines are, respectively, for the advection and stretching terms involving mean fields.

Vertically Averaged

$$\frac{\partial \bar{B}_x}{\partial t} = -\partial_z \mathcal{E}_y + \bar{B}_z \partial_z \bar{U}_x - \bar{U}_z \partial_z \bar{B}_x,$$

$$\frac{\partial \bar{B}_y}{\partial t} = S\bar{B}_x + \partial_z \mathcal{E}_x + \bar{B}_z \partial_z \bar{U}_y - \bar{U}_z \partial_z \bar{B}_y,$$

Horizontally Averaged

$$\frac{\partial \bar{B}_y}{\partial t} = -\partial_x \mathcal{E}_z + \bar{B}_x \partial_x \bar{U}_y - \bar{U}_x \partial_x \bar{B}_y,$$

$$\frac{\partial \bar{B}_z}{\partial t} = \partial_x \mathcal{E}_y + \bar{B}_x \partial_x \bar{U}_z - \bar{U}_x \partial_x \bar{B}_z.$$

Large Scale Dynamos in Shearing Box MRI Simulations

Cycle periods in shearing box MRI stratified simulation, (outflow bdry in z)
(Simon et al. 2011)

(parameterized MFD model; volume averaged $\alpha_2 = -0.01 \Omega H$)

$$\frac{d\langle B_y \rangle}{dt} = -q\Omega \langle B_x \rangle - \frac{|v_A|}{2H} \langle B_y \rangle + \frac{\alpha_1}{2H} \langle B_x \rangle,$$

$$\frac{d\langle B_x \rangle}{dt} = -\frac{|v_A|}{2H} \langle B_x \rangle - \frac{\alpha_2}{2H} \langle B_y \rangle.$$

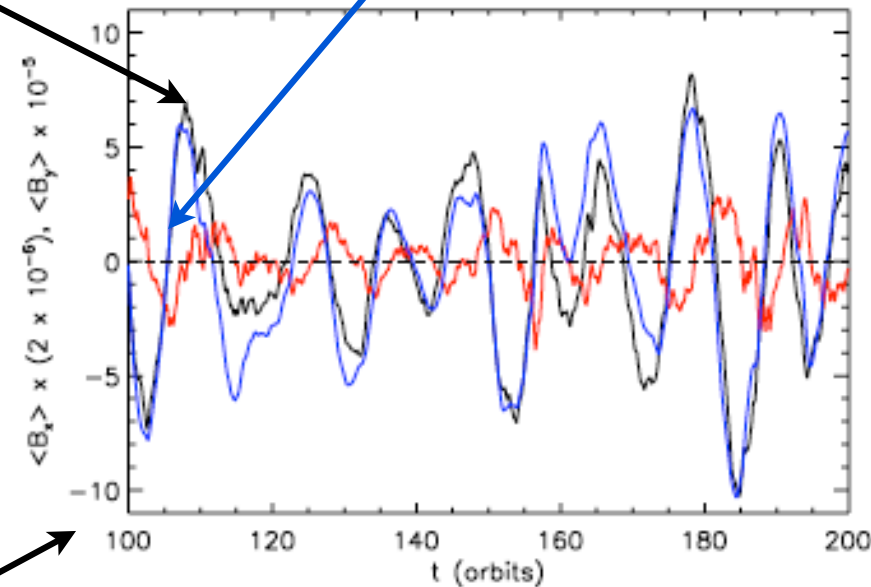
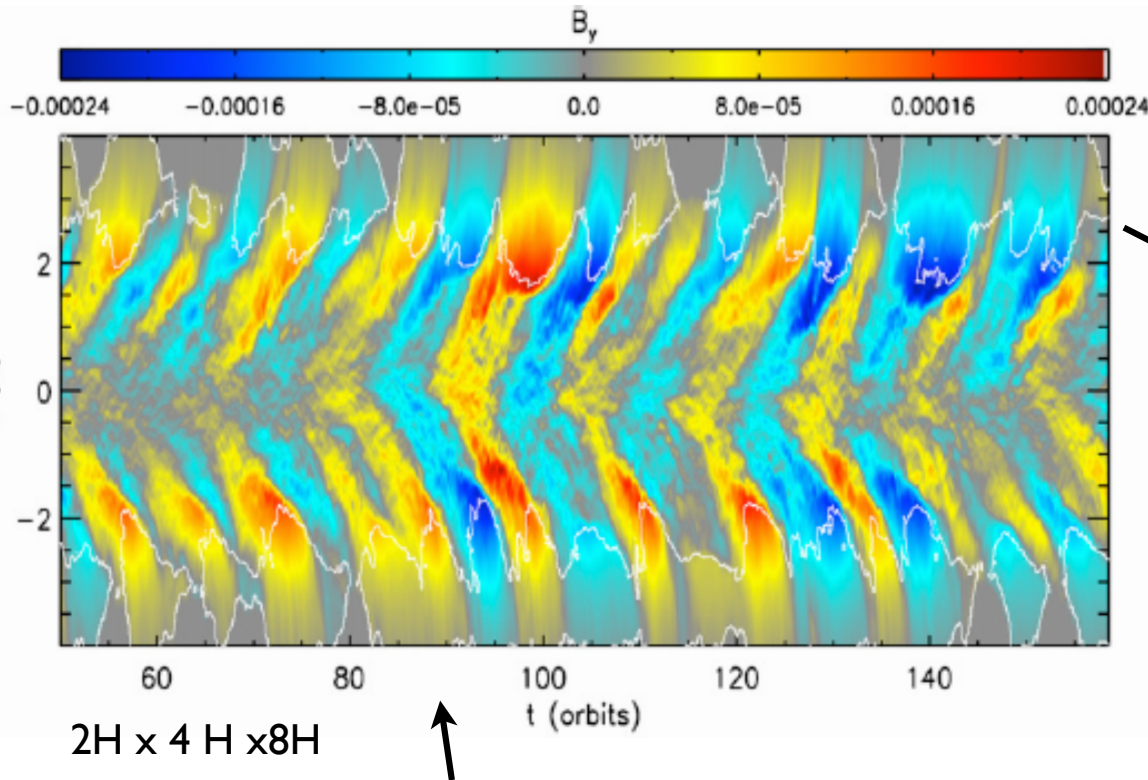


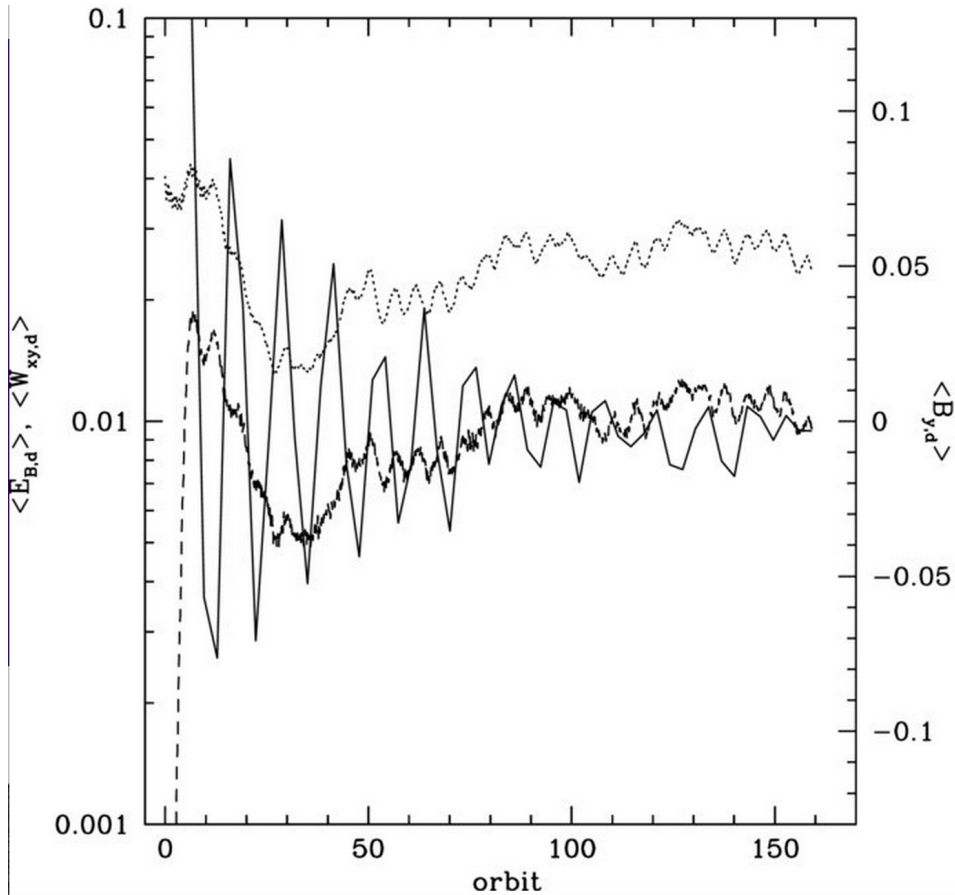
Figure 7. Time evolution of volume-averaged field components for part of 32Num. Red is $\langle B_x \rangle$, black is $\langle B_y \rangle$, and blue is $\langle B_y \rangle$ as calculated from $\langle B_x \rangle$ using a simple α - Ω dynamo model discussed in the text. The volume average is done for all x and y and for $|z| \leq 0.5H$. The dashed line corresponds to $\langle B_{x,y} \rangle = 0$. $\langle B_x \rangle$ has been multiplied by a factor of five relative to $\langle B_y \rangle$ to make a more direct comparison possible. The variations in $\langle B_x \rangle$ are accompanied by variations in $\langle B_y \rangle$, which are offset in time, and the dynamo model shows that the evolution of $\langle B_y \rangle$ is controlled by the shear of the radial field and the buoyant removal of the toroidal field.

horizontally averaged

volume averaged

(also Brandenbug et al. 1995; Ogilvie & Lesur 2008; Davis et al. 2010; Shi et al. 16)

Correlation of Stress with Large Scale Fields



Guan and Gammie (2011)

Oscillation period for $\langle B_y \rangle$ (solid) is twice that of Magnetic energy density $\langle E_B \rangle$ (dotted) and stress $\langle W_{xy} \rangle$ (dashed) Note: initially $\beta = 25$ with initial net toroidal field; **box averages**

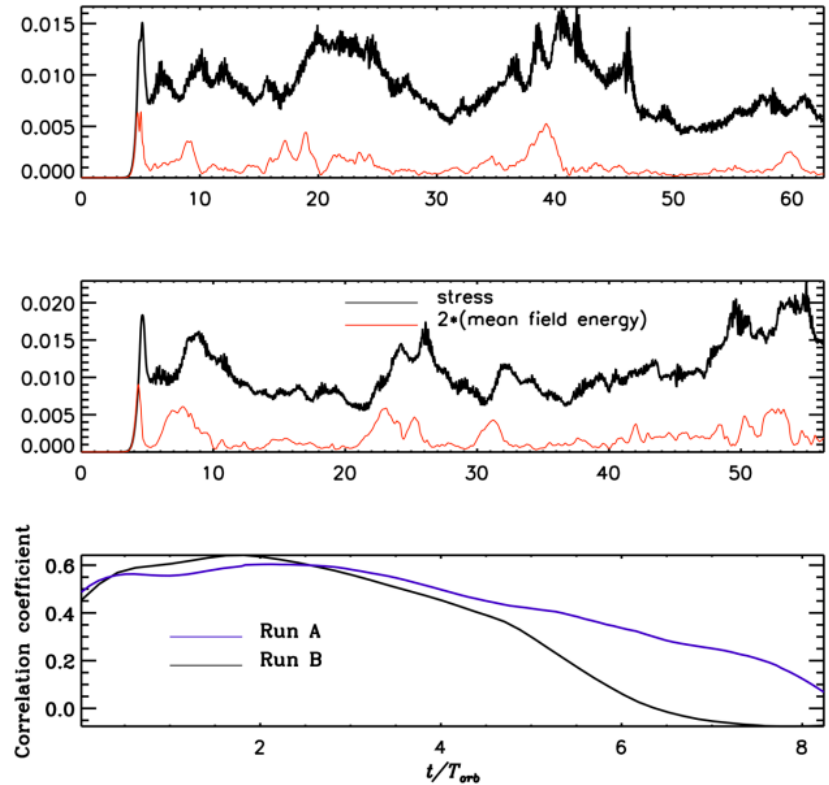
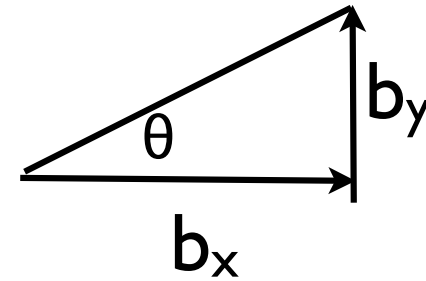


Figure 9. We show here the evolution of the stresses and the large-scale fields and the correlation between them. Top panel is for Run A and the middle panel is for Run B. In the bottom panel, we show the correlation coefficient as a function of time.

Bhat et al. (2016) (planar averages, horizontal shown, early times)

$\alpha_{ss}\beta = \text{constant}$

Constant $K = \alpha_{ss}\beta$ is equivalent to constant field tilt angle since:

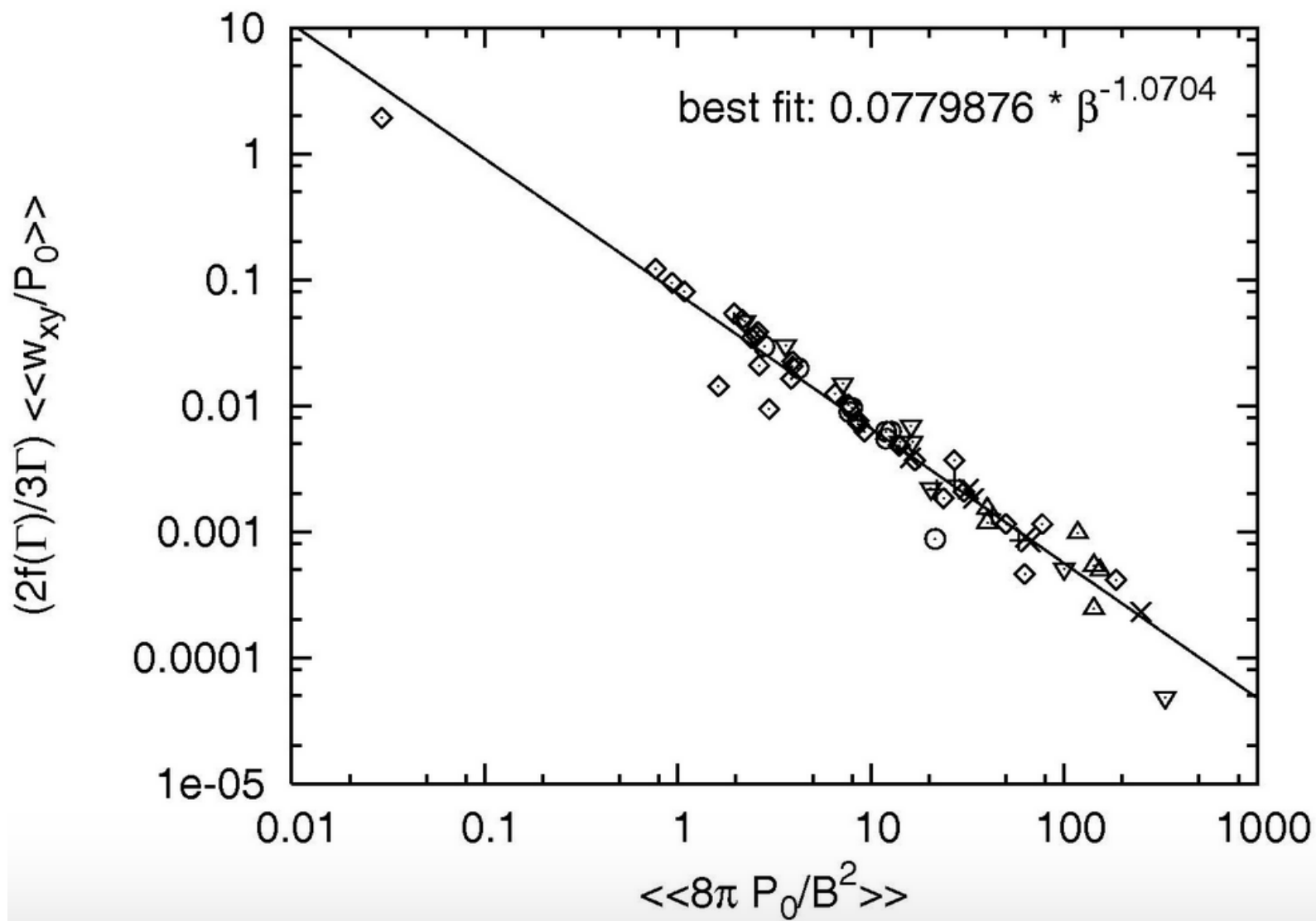


$$\alpha_{ss} \simeq \frac{\langle b^2 \rangle \langle b_x b_y \rangle}{P \langle b^2 \rangle}$$
$$= \beta^{-1} \frac{\tan \theta}{(1 + \tan^2 \theta + b_z^2 / b_x^2)} \sim \beta^{-1} \frac{\tan \theta}{1 + \tan^2 \theta}; \quad (\tan \theta \equiv b_y / b_x)$$

$|b_y| \sim |b_x|(1 + q\Omega\tau_c)$ implying that $\tan \theta \sim 1/(1 + q\Omega\tau_c)$

- expect $\frac{b_x / b_y}{\langle B_x \rangle / \langle B_y \rangle} \ll 1$

because azimuthal mean field can be stretched over a diffusion time which is \gg correlation time



Blackman, Penna & Varniere (2006)

FIG. 1. Isothermal data of Table 8, Table 9 and Table 10 and best fit lines. Top row: $\text{Log } \alpha_{xy}(P_0)$ and $\text{Log } \alpha_{xy}(P_0)$ vs. $\text{Log } \beta(P_0)$, respectively.

Tilt angle constant even for different shear profiles.
 Explanation: correlation time decreases with shear

$$\text{ACF}(B_i(\delta\mathbf{x})) = \left\langle \frac{\int B_i(\mathbf{x} + \delta\mathbf{x}, t) B_i(\mathbf{x}, t) d^3\mathbf{x}}{\int B_i^2(\mathbf{x}, t) d^3\mathbf{x}} \right\rangle$$

ACF(B)

$$B_y \sim -q\Omega\tau B_x,$$

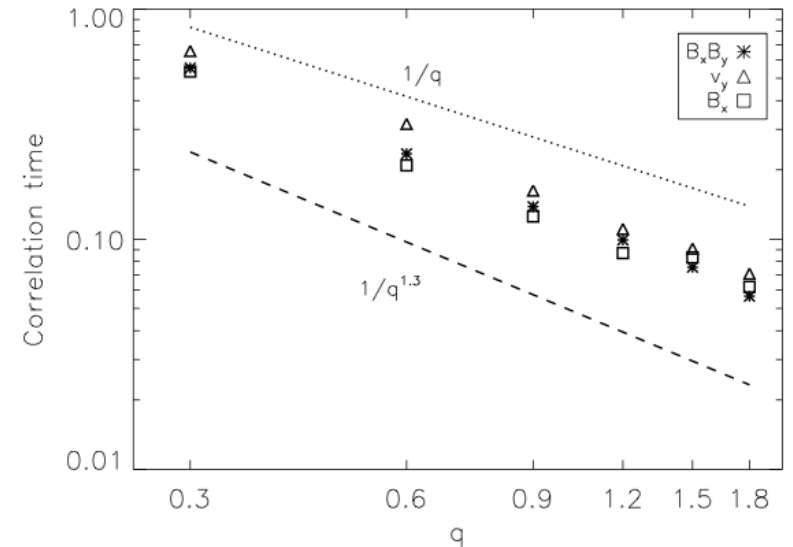
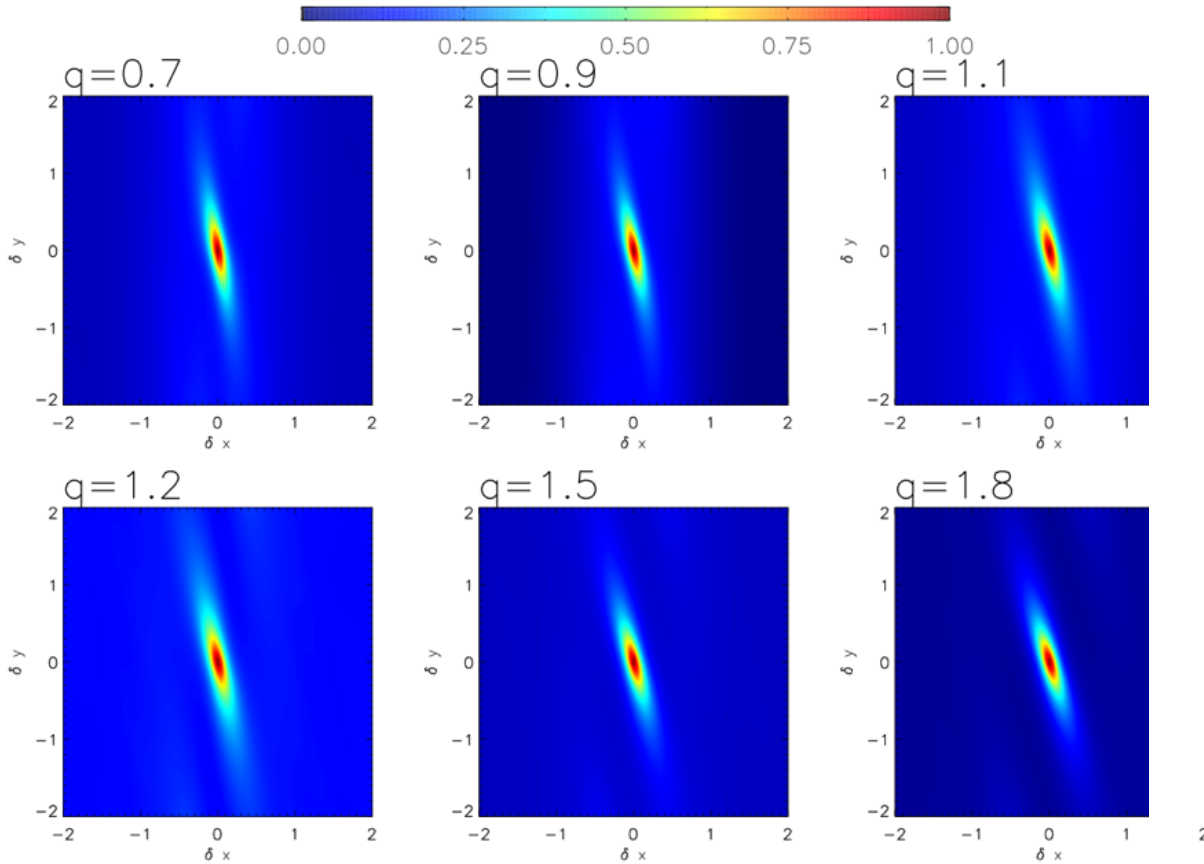


Figure 13. Log-log plot for $\beta = 100$ runs showing correlation time for v_y (diamonds), $B_x B_y$ (asterisks) and B_x (squares) calculated by an exponential fit. The dotted line shows the $1/q$ fit, while the dashed line the $1/q^{1.3}$ fit.

Nauman & Blackman 14;
 Blackman & Nauman 15

- highlights that linear terms dominate nonlinear terms in B_y
- not true in Rayleigh regime ($q > 2$; NB 15)

- Overall interpretation of simulations hints toward of large scale, nonlocal transport

REFERENCE	Evidence for large scale transport or correlation with large scale fields
LOCAL SIMULATIONS	
Hawley et al. (1995); Lesur & Longaretti (2011)	Energy power spectra in the disk dominated by domain scale.
Bai & Stone (2013)	For $\beta < 10^3$, both disk and corona dominated by $\overline{B_r B_\phi}$;
Nauman & Blackman (2014)	Stress spectra in disk and corona dominated by nearly domain scale ($\sim H$).
Bhat et al. (2016)	large scale dynamo precedes turbulence / stress correlates with large scale fields .
GLOBAL SIMULATIONS	
Beckwith et al. (2011); Flock et al. (2012); Suzuki & Inutsuka (2014)	Azimuthal power spectra in the disk dominated by domain scale ($\sim R$).
Guan & Gammie (2011); Flock et al. (2012); Parkin (2014a)	$\overline{B_\phi}$ shows system scale dynamo cycle periods and $\mathcal{E}_\phi \sim \alpha_{\text{dyn}} \overline{B_\phi}$
Suzuki & Inutsuka (2014); Zhu & Stone (2017)	Stress and torque dominated by $\overline{B_r B_\phi}$ in the corona even for $\beta \sim 10^3 - 10^5$; Weak vertical transport and outflow

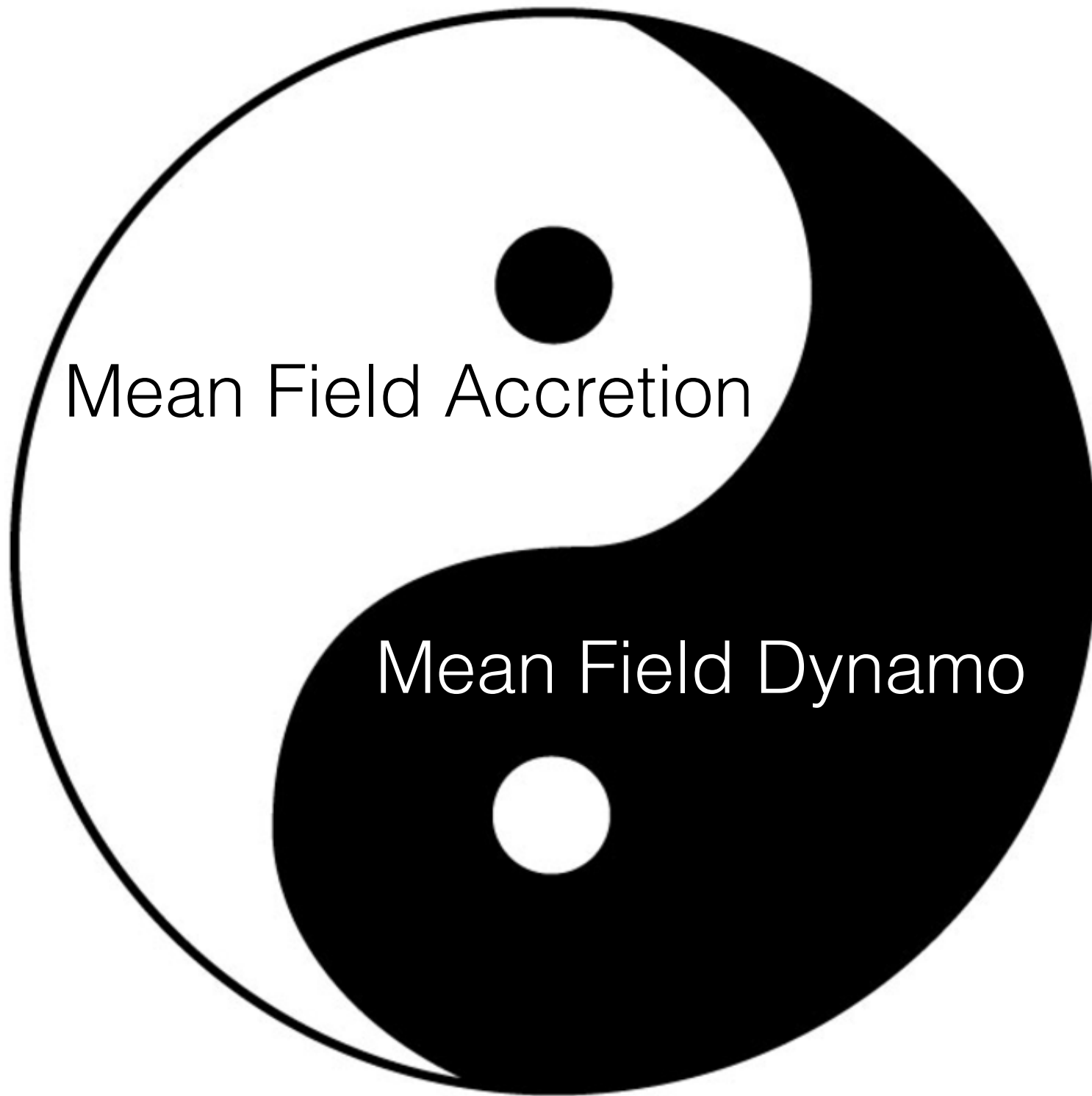
(B. & Nauman 2015; Nauman & B in prep.)

Of particular note is the dominance of accretion torque (and accretion rate) by non-local coronal transport in recent global sims (Zhu & Stone 2017)

$$\overline{B_r B_\phi}$$

Large Scale Dynamo Theory and Accretion Theory Should be Unified

- large scale fields from MRI **(1)** precede turbulent growth (Ebrahimi and B 16; Bhat et al. 16) and **(2)** are sustained during turbulence (Brandenberg et al. 95 etc...to present)
- Large scale fields come from some combination of large scale dynamo generation and advection that overcomes diffusion (or balances in steady state); both of these
- Question of whether fields advect or diffuse is only part of the story for mean field theory as growth term not only diffusion terms.
- ultimately: **mean field accretion disk theory and mean field dynamo theory are complementary components of what should be a single theory**
- accretion disk dynamos likely not driven by kinetic helicity but by **current helicity along with helicity fluxes to corona (B2005;B&Park 2012; Vishniac 2009 +..)**
- non-axisymmetric perturbations that supply small scale current helicity seem to be underlying what we find in Ebrahimi & Blackman (2016) (ongoing)
- **Ask not “is mean field theory correct?” but “do we have the correct mean field theory?”**



Mean Field Accretion

Mean Field Dynamo

Relevance of Magnetic Helicity

- measures linkage, twist, and writhe of flux bundles
- ideal MHD with $\mathbf{v}=0$: magnetic energy minimized for force free fields (Woltjer 58); helicity on largest scale subj. to B.C.
- more complicated w/flows (e.g. Woltjer 58b) **BUT KEY POINT: energy $\sim kH_M$ minimized by low k at fixed H_M**
- **magnetic helicity better conserved than mag. energy** for most realistic systems (Taylor 74,86); can quantify the veracity of this for arbitrary spectra (B04,09):

$$\frac{\text{magnetic energy decay term}}{\text{magnetic helicity decay term}} \sim \frac{v_M \mathbf{J}^2}{v_M (\mathbf{J} \cdot \mathbf{B})} \propto \frac{1}{L}$$

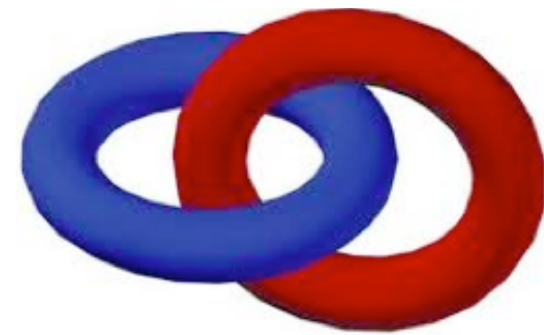
\Rightarrow So as structures go to smaller scales, magnetic energy dissipation increases faster with decreasing scale

- field aligned EMF implies source of large and small scale helicity or helicity fluxes in steady state even if total vanishes:

$$\partial_t \langle \mathbf{A} \cdot \mathbf{B} \rangle = -2 \langle \mathbf{E} \cdot \mathbf{B} \rangle - \langle \nabla \cdot (2 \times \mathbf{A} - \mathbf{A} \times \partial_t \mathbf{A}) \rangle$$

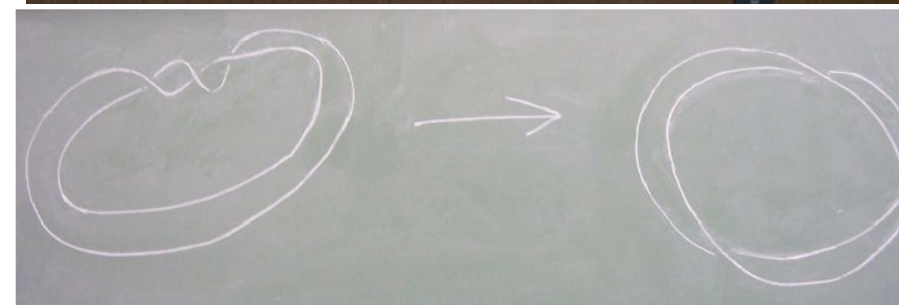
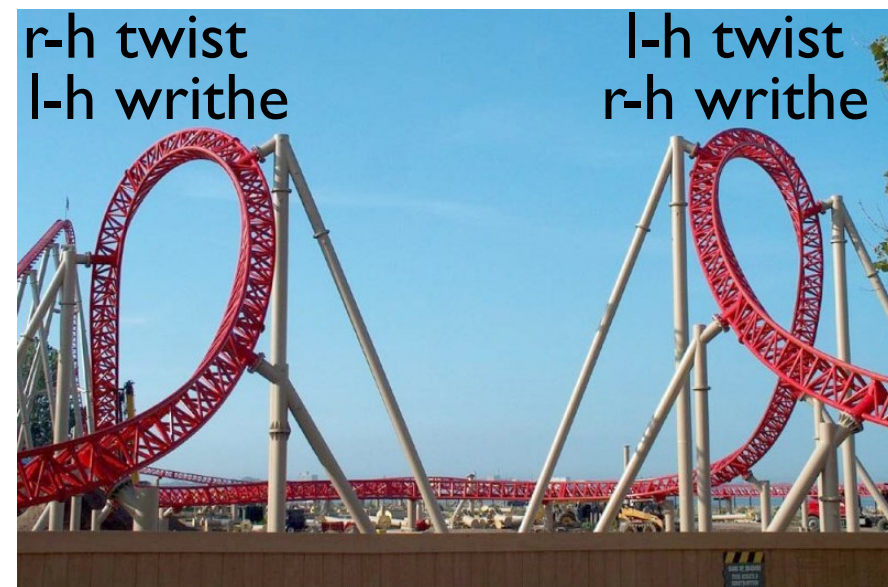
$$\partial_t \langle \bar{\mathbf{A}} \cdot \bar{\mathbf{B}} \rangle = -2 \langle \bar{\mathbf{E}} \cdot \bar{\mathbf{B}} \rangle - \langle \nabla \cdot (2 \mathbf{E} \times \mathbf{A} - \mathbf{A} \times \partial_t \mathbf{A}) \rangle$$

$$\partial_t \langle \mathbf{a} \cdot \mathbf{b} \rangle = -2 \langle \mathbf{e} \cdot \mathbf{b} \rangle - \langle \nabla \cdot (2 \mathbf{e} \times \mathbf{a} - \mathbf{e} \times \partial_t \mathbf{a}) \rangle$$



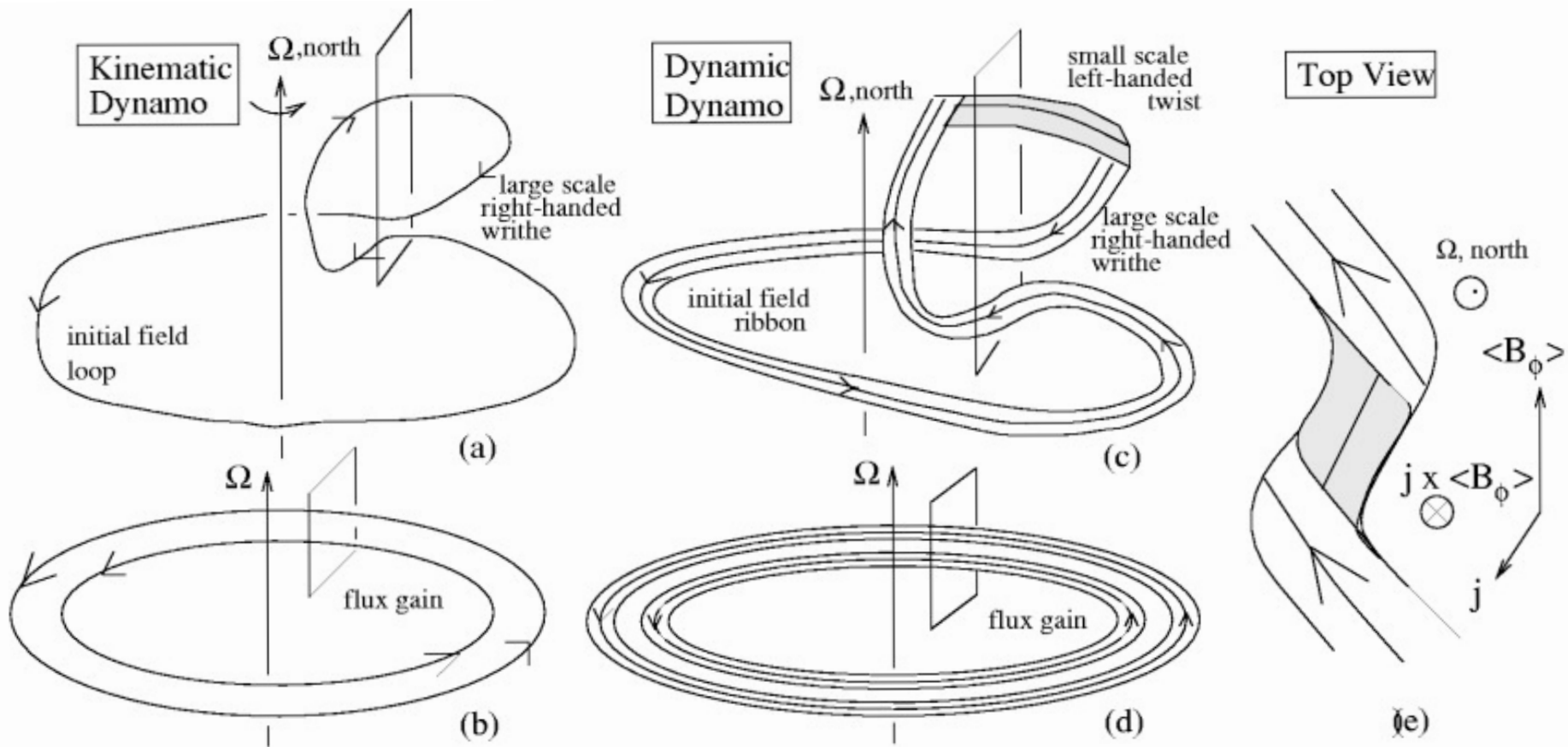
$$H_M = \int \mathbf{A} \cdot \mathbf{B} dV = 2 \int A_1 B_1 dl_1 dA_1$$

$$= 2 \int B_2 B_1 dA_2 dA_1 = 2 \phi \cdot \phi$$



Revising “ α - Ω ”-LSD picture with open boundary:

Expect both signs of helicity in both hemispheres with North (South):
large scale having “+(-)” sign and small scale “- (+)” sign.



LSD from MRI in shearing box with initial zero mean field, open boundaries (Gressel 2010)

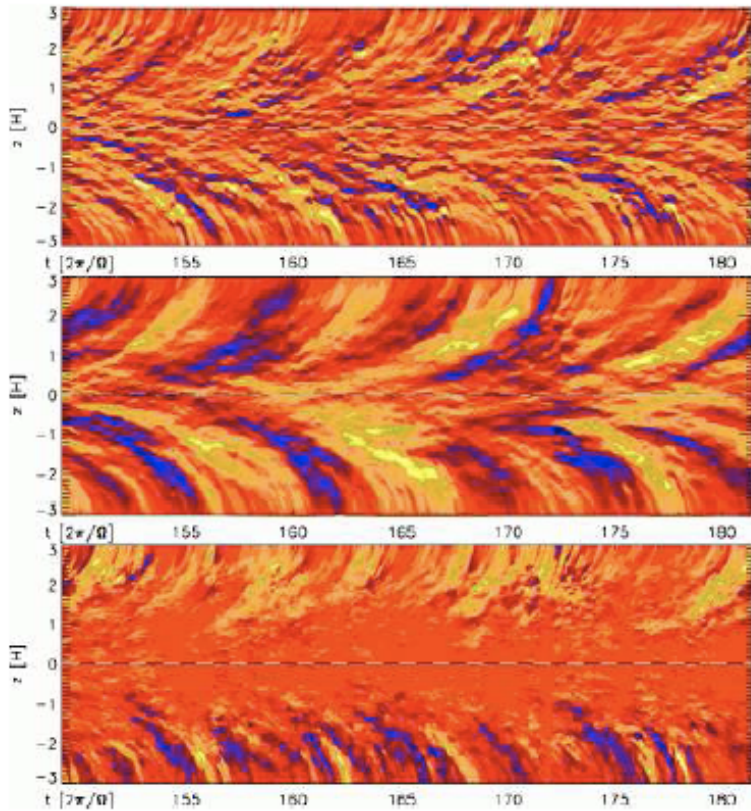


Figure 1. Space time evolution of the horizontally averaged radial field $\bar{B}_x(z, t)$, azimuthal field $\bar{B}_y(z, t)$, and magnetic α effect (cf. Sec. 4.1). The colour coding is normalised by the vertical rms amplitude at any given time to remove the stochastic fluctuations in the overall field strength and highlight the coherent pattern.

- Flow driven by shear with stratification (isothermal, outflow bdry); **horizontal averages**
- EMF sign consistent with current helicity NOT kinetic helicity

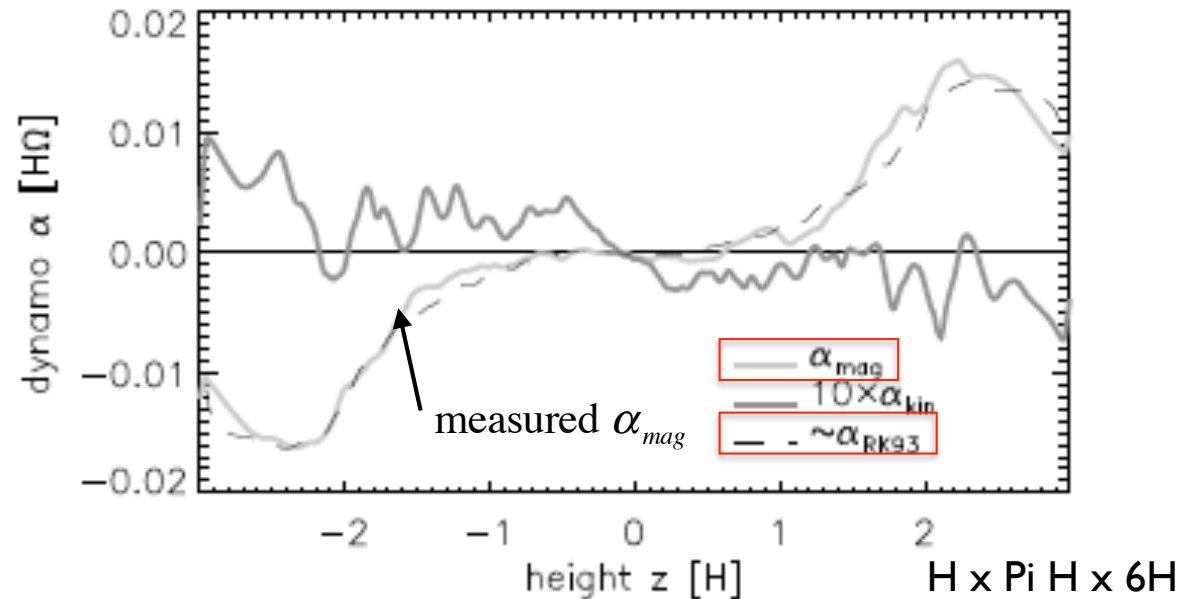


Figure 3. Helical α effect based on the current helicity (light grey) and kinetic helicity (dark grey). Both quantities are highly fluctuating in time but show a systematic average which follows the shape (dashed line) of the effect predicted for stratified, rotating turbulence by RK93.

$$\partial_t \bar{B}_y = \partial_z \bar{\mathcal{E}}_x - q\Omega \bar{B}_x$$

$$\partial_t \bar{B}_x = -\partial_z \bar{\mathcal{E}}_y$$

$$\bar{\mathcal{E}}_y = \langle \mathbf{v} \times \mathbf{b} \rangle_y = \alpha_{yy} B_y + \eta_T \partial_z B_x$$

$$\alpha_{yy} = \alpha_{mag} + \alpha_{kin}$$

$$\propto \langle \mathbf{b} \cdot \nabla \times \mathbf{b} \rangle - \langle \mathbf{v} \cdot \nabla \times \mathbf{v} \rangle \sim \langle \mathbf{b} \cdot \nabla \times \mathbf{b} \rangle;$$

Turbulent Diffusion and Helicity

- Advection, diffusion, and growth all compete in accretion disks general—not just diffusion and advection
- Imagine a closed volume with an initial large magnetic field of large scale.
- In context of a periodic box, for example, consider large scale to be $k=1$, as $k=0$ cannot evolve
- Force the system with non-helical velocities, with $|v| \geq |B|$ at $k \gg 1$, and ruminates: what happens to the large scale field?

Helical Fields Diffuse Much Less Efficiently Than Nonhelical Fields

- Turbulent diffusion of large scale helicity must grow some small scale helicity, but growth small scale helicity fights the diffusion because it acts as a growth term for large scale helicity!
- Remember that magnetic helicity, if left alone, will relax to the largest state as that minimizes the energy; diffusing to small scales is not favorable if there is too much helicity in the system
- Above a modest threshold, large scale magnetic helicity it will turbulently decay only on microphysically slow time scales

Look first at Large Scale Magnetic Energy Evolution

$$\partial_t \mathbf{B} = \nabla \times (\mathbf{v} \times \mathbf{B}) + \nu_M \nabla^2 \mathbf{B}$$

$$\mathbf{B} = \mathbf{b} + \bar{\mathbf{B}}$$

$$\Rightarrow \partial_t \bar{\mathbf{B}} = \nabla \times \bar{\mathbf{e}} + \nu_M \nabla^2 \bar{\mathbf{B}}$$

$$\bar{\mathbf{e}} \equiv \langle \mathbf{v} \times \mathbf{b} \rangle = \alpha \bar{\mathbf{B}} - \beta \nabla \times \bar{\mathbf{B}} + ..$$

(Ignoring divergence terms for the moment, assuming in closed volume)

$$\Rightarrow \frac{1}{2} \partial_t \bar{\mathbf{B}}^2 = \bar{\mathbf{B}} \cdot \nabla \times \bar{\mathbf{e}} + \nu_M \nabla^2 \bar{\mathbf{B}} = \alpha \langle \bar{\mathbf{B}} \cdot \nabla \times \bar{\mathbf{B}} \rangle - (\beta + \nu_M) \langle (\nabla \times \bar{\mathbf{B}})^2 \rangle,$$

Not decay

Decay term

$$\bar{\mathbf{B}} = \nabla \times \bar{\mathbf{A}}$$

$$\langle \bar{\mathbf{B}} \cdot \nabla \times \bar{\mathbf{B}} \rangle = -k_1^2 \langle \bar{\mathbf{A}} \cdot \bar{\mathbf{B}} \rangle \text{ in Colomb gauge}$$

(and gauge invariant for present case for which flux terms vanish)

MAGNETIC HELICITY: has to be dealt with

Equations for Our Turbulent Diffusion Problem

$$\begin{aligned}
 \partial_t \bar{\mathcal{E}} &= \overline{\partial_t \mathbf{v} \times \mathbf{b}} + \overline{\mathbf{v} \times \partial_t \mathbf{b}} \\
 &= \frac{1}{3} (\overline{\mathbf{b} \cdot \nabla \times \mathbf{b}} - \overline{\mathbf{v} \cdot \nabla \times \mathbf{v}}) \bar{\mathbf{B}} - \frac{1}{3} \overline{v_2^2} \nabla \times \bar{\mathbf{B}} - \frac{\bar{\mathcal{E}}}{\tau} \\
 &\quad \alpha \qquad \qquad \qquad \beta \\
 \Rightarrow \bar{\mathcal{E}} &\approx \frac{\tau}{3} (k_2^2 \overline{\mathbf{a} \cdot \mathbf{b}} - \overline{k_2^2 \mathbf{v} \cdot \nabla \times \mathbf{v}}) \bar{\mathbf{B}} - \frac{\tau}{3} \overline{v_2^2} \nabla \times \bar{\mathbf{B}}
 \end{aligned}$$

$$\partial_t B_1^2 = 2 \frac{\tau}{3} (k_2^2 H_2^M - \cancel{H_2^V}) \frac{k_1^2 H_1^M}{4\pi\rho} - 2 \left(\frac{\tau}{3} v_2^2 + v_M \right) k_1^2 \bar{B}_1^2 + \cancel{\nabla \cdot \langle Q_1 \rangle} \quad (1)$$

$$\partial_t H_1^M = 2 \frac{\tau}{3} (k_2^2 H_2^M - \cancel{H_2^V}) \frac{B_1^2}{4\pi\rho} - 2 \left(\frac{\tau}{3} v_2^2 + v_M \right) k_1^2 H_1^M + \cancel{\nabla \cdot \langle Q_1 \rangle} \quad (2)$$

$$\partial_t H_2^M = -2 \frac{\tau}{3} (k_2^2 H_2^M - \cancel{H_2^V}) \frac{B_1^2}{4\pi\rho} + 2 \frac{\tau}{3} v_2^2 k_1^2 H_1^M - 2 v_M k_2^2 H_2^M + \cancel{\nabla \cdot \langle Q_M \rangle} \quad (3)$$

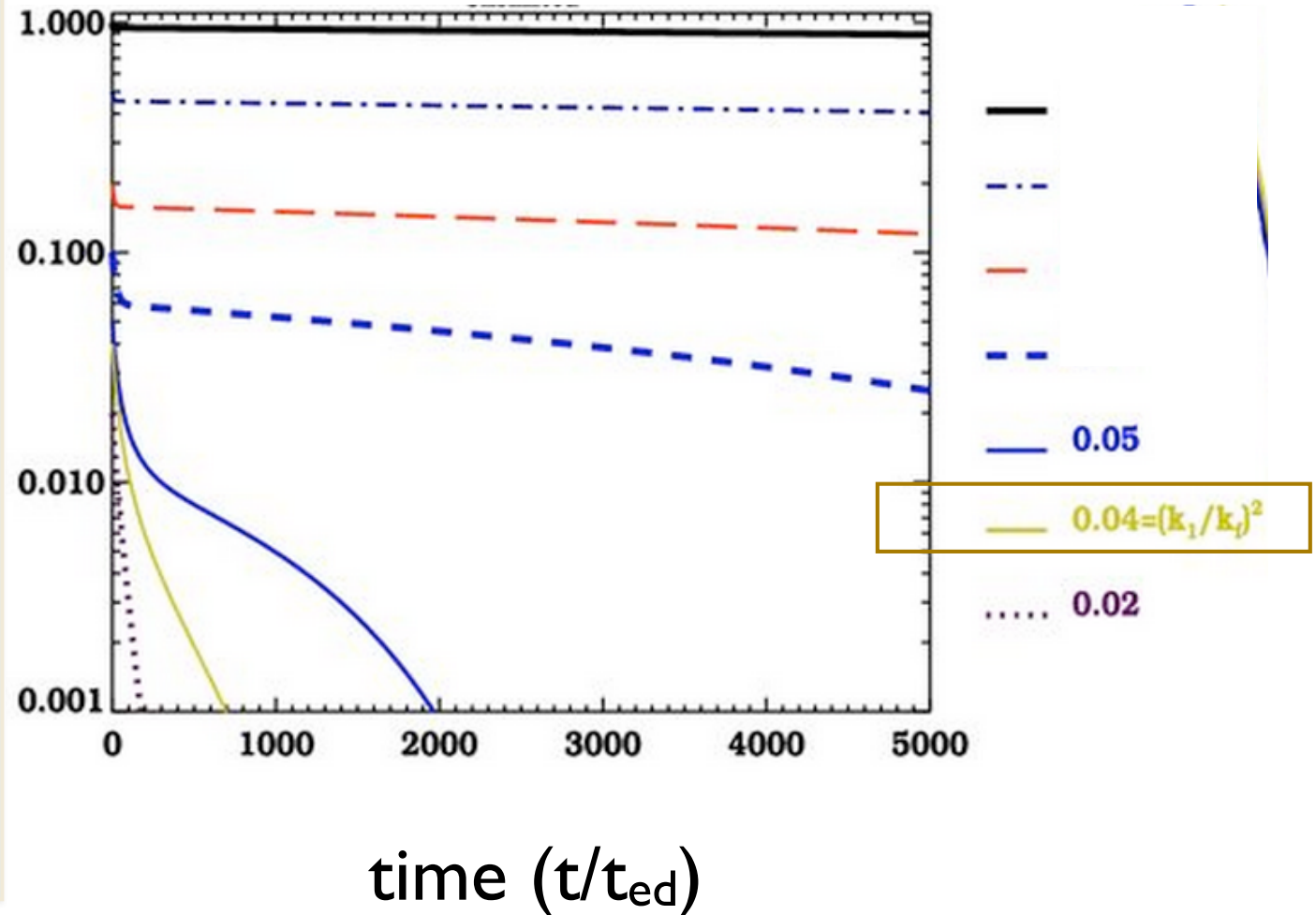
$$\partial_t E_2^V = 0$$

- Closed system of equations, when forced with non-helical turbulence
- For fully helical large scale field, (1) and (2) are same

Resilience of Helical Field to Turbulent Diffusion

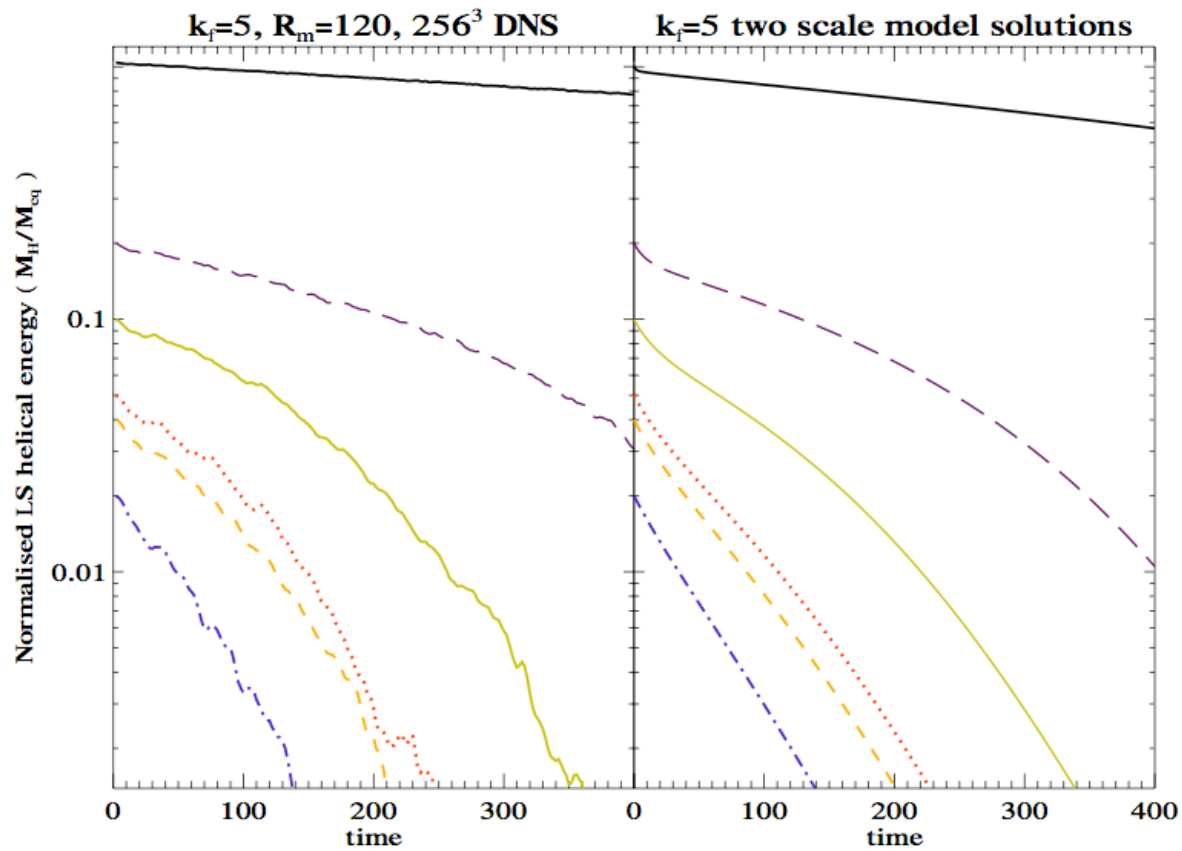
Normalized helical large-scale magnetic energy in units of turbulent kinetic energy $M_H/M_{eq,v}$ (2-scale theory, $R_M=12000$, $k_f=5$)

Since critical helical magnetic energy fraction of equipartition with turbulence to incur slow decay is $(k_1/k_2)^2$, even a range of sub equipartition helical fields just evolve resistively despite presence of vigorous turbulence



LS helical magnetic energy

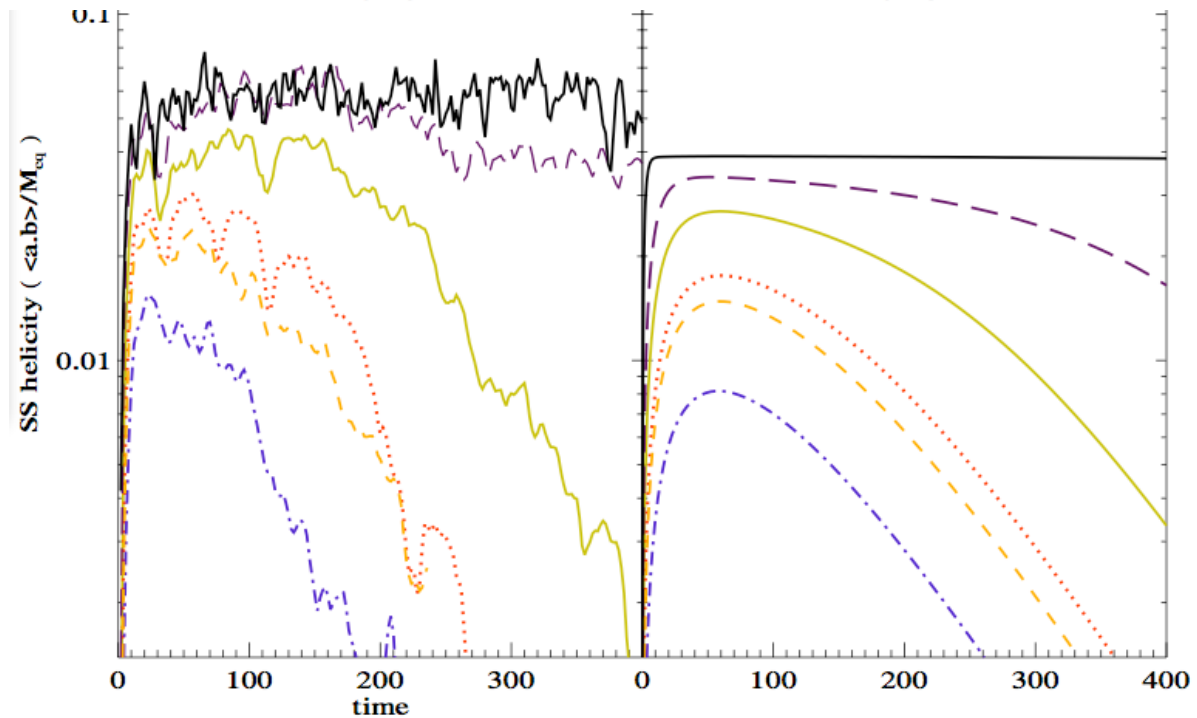
$$\frac{M_{H,1}}{M_{eq,v}}$$



Bhat et al. (2014)
 Periodic box,
 simulations using
 Pencil Code
 forced at $k=k_f$
 with non-helical
 isotropic velocity.

SS helicity

$$\frac{|\langle \mathbf{a} \cdot \mathbf{b} \rangle|}{M_{eq,v} / k_1}$$



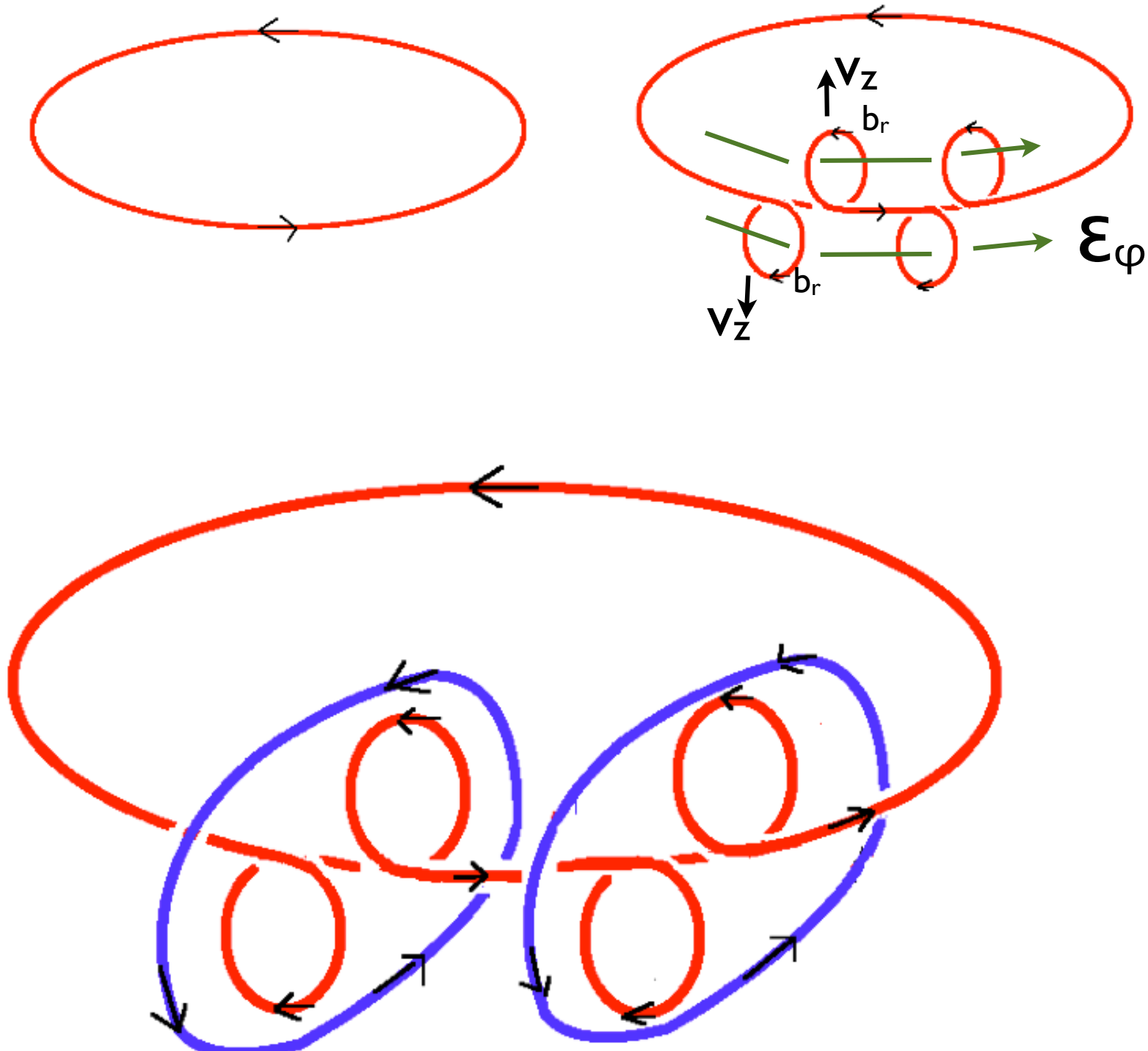
Implications taken at face value

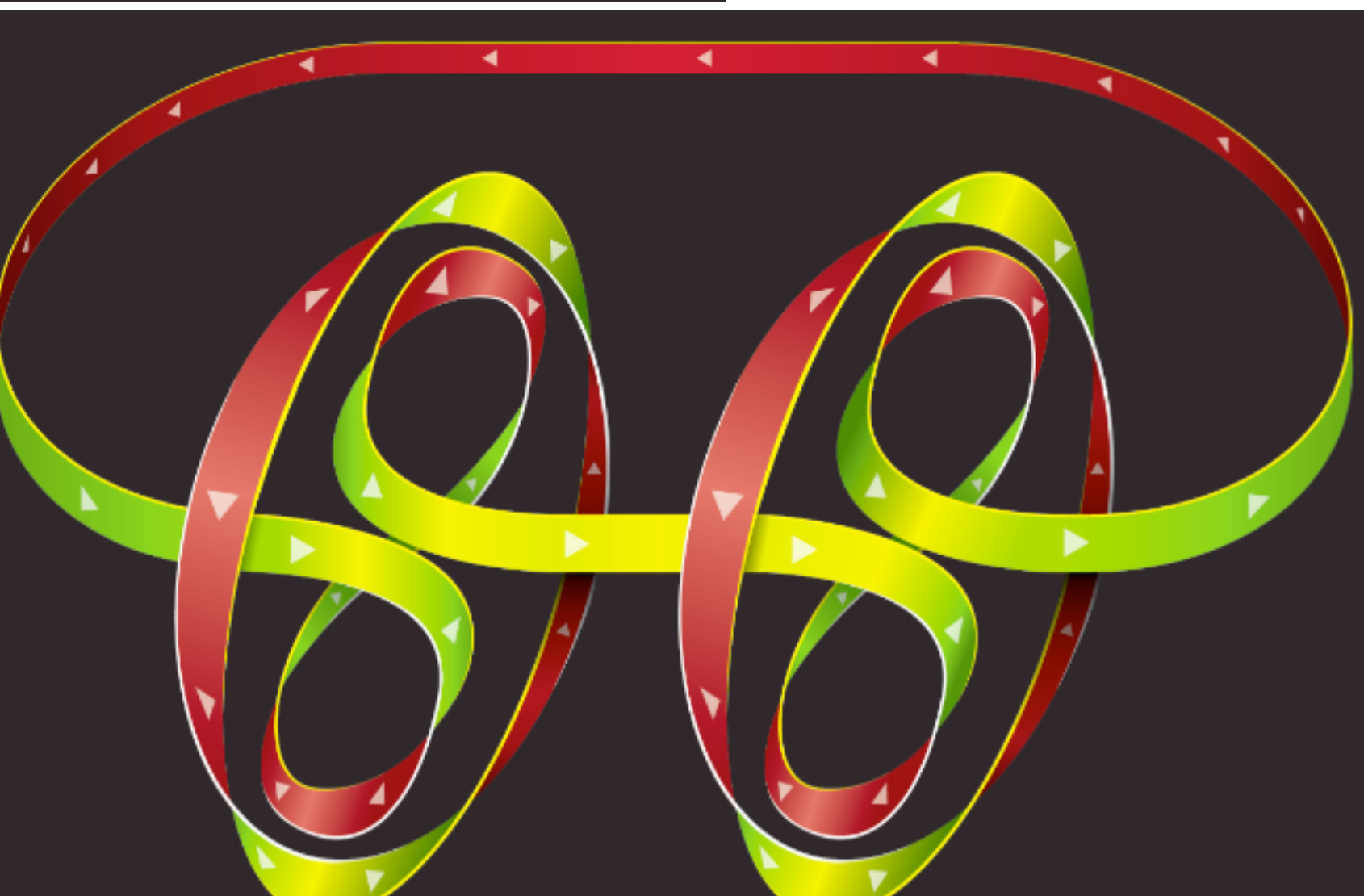
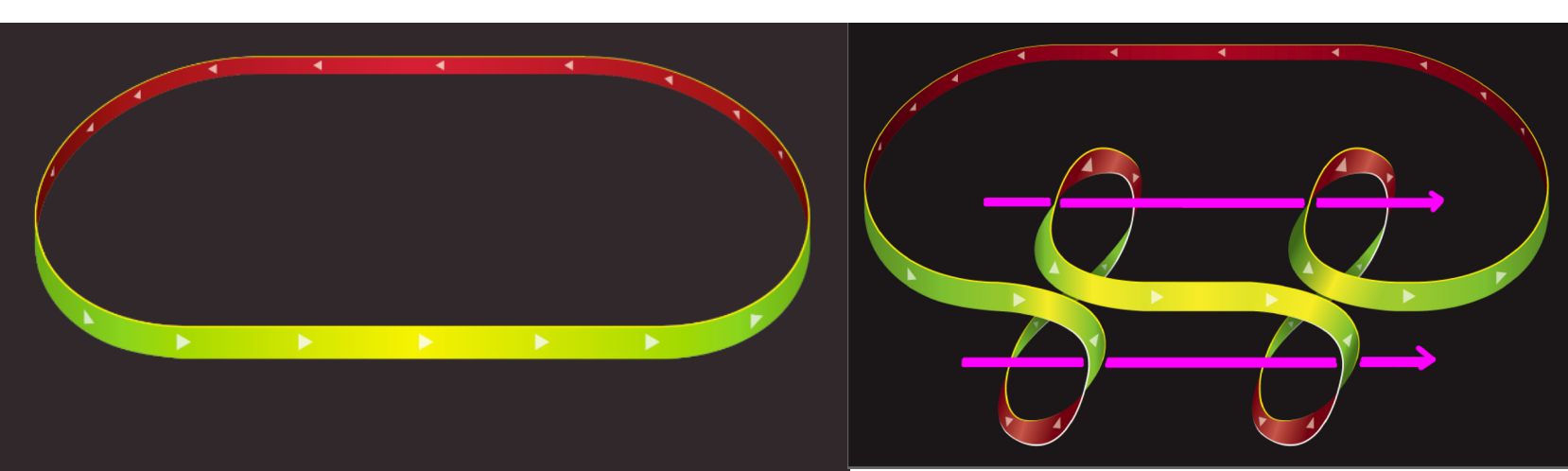
- advection/generation of large scale magnetic fields in accretion disks (long standing controversy would depend on helical vs. non-helical nature of field being advected)
- Helical fields in jets would not be evidence for magnetically dominated systems: we have just seen sub-equipartition helical fields survive turbulent diffusion. Thus jets could be turbulent and still support mean helical field
- Caveats: helicity fluxes

Conclusions/Challenges

- Observations and both local and global simulations suggest ionized disk transport may be dominated by non-local magnetic phenomena even if MRI is operative:
- Large scale dynamos ubiquitously seen in MRI simulations both before turbulence and after saturation may be important contributors to stress and saturation and so we'd like to understand how they operate and their connection to the stress.
- Contemplate that large scale dynamos and disk accretion theory are artificially decoupled components of a single unified theory and combining the two will ultimately help to better self-consistently predict disk, corona and jet powers for a given set of inputs (e.g. accretion rate).
- More feedback toward putting the pieces together is needed between simulation and theory to improving practical “textbook” accretion theory (i.e. improve the physics but remain practical for modelers)
- A mean magnetic field aligned $\langle \mathbf{v} \times \mathbf{b} \rangle_{\parallel}$ is fundamental for explaining large scale field growth and sustenance in most all known circumstances and points to some role of magnetic helicity
- Magnetic helicity plays a role even in the basic physics of turbulent diffusion: helical fields diffuse much less efficiently.
- Fraction of transport allocated to disc vs. coroneae may have to do with the spectral produces by the MRI in the disk: only fields of large enough scale or with sufficient helicity buoyantly escape on a turbulent diffusion time seed coronal transport, magnetic relaxation in the corona subject to foot point motion then leads to further relaxation to open lines up to jet.
- Physical principles beyond parameters are needed to better delineate these disk, coronal, and jet fractions and still useful to consider simplified models to get at these principles.

Magnetic field schematics in most all textbooks DO NOT CONSERVE MAGNETIC HELICITY:





Black
Blackman &
Hubbard
2014